RSC Sustainability

ROYAL SOCIETY OF CHEMISTRY

CRITICAL REVIEW

View Article Online
View Journal | View Issue

Cite this: *RSC Sustainability*, 2025, **3**, 2472

Insights into hierarchical porous titanium(IV) phosphonates: synthesis, structure & applications

Archana K. Pattnaik, [a] Gobinda Chandra Behera [b] and Kulamani Parida *[a]

Hierarchically porous titanium(IV) phosphonates (HPTPs) have recently attracted significant attention as a novel class of hybrid materials that achieve remarkable flexibility in structural porosity, chemical strength, and multifunctionality, offering broad applicability compared to traditional hybrid materials. Unlike carboxylate-based metal–organic frameworks (MOFs), they exhibit robust hydrolytic stability due to their multimodal coordinating ability and strong Ti–O–P bonding. This makes them suitable candidates for catalysis, pollutant adsorption, ion exchange, and energy storage. However, despite their promising capabilities, the unpredictable self-assembly of Ti(IV) metal nodes, poor structural crystallinity, and challenges in hierarchical pore size control hinder the tunability of these materials for targeted applications. Furthermore, the relationships between porosity, stability, and catalytic efficiency necessitate further research to improve overall performance. This review critically examines synthetic methodologies, structural features, and emerging applications of HPTPs, highlighting strategies to address these limitations. Despite advancements in synthetic procedures, the crystallization of HPTPs with precise pore topology and desirable electronic characteristics remains challenging. The combination of computational modeling and machine learning may enhance material design, stability, and porosity. Additionally, solventless strategies alongside green fabrication and nanomaterial integration, could further expand the potential applications of HPTPs in energy storage, photocatalysis, and wastewater treatment, paving the way for industrial-scale utilization.

Received 3rd February 2025
Accepted 13th April 2025

DOI: 10.1039/d5su00074b

rsc.li/rscsus

[a]*Centre for Nanoscience and Nanotechnology, Siksha 'O' Anusandhan (Deemed to be University), Bhubaneswar 751030, Odisha, India. E-mail: kulamaniparida@soa.ac.in; arcpattnaik@gmail.com; akp18@iitbbs.ac.in*

[b]*Department of Chemistry, Maharaja Purna Chandra Autonomous College, Takhatpur, Baripada 757003, Odisha, India. E-mail: bcgobind@gmail.com*

Archana K. Pattnaik

Dr Archana K. Pattnaik is a postdoctoral fellow at the Centre for Nanoscience and Nanotechnology, Siksha 'O' Anusandhan (Deemed to be University). Her research focuses on the design and fabrication of single-crystal functional materials such as APIs, co-crystals, ionic liquids, MOFs, COFs, and POFs for applications in biomedical engineering, environmental remediation, and energy materials. She specializes in supramolecular and solid-state structural chemistry with an emphasis on structure–property relationships. Dr Pattnaik earned her PhD from IIT Bhubaneswar, where she studied isomorphous and isostructural coordination polymers and MOFs based on organophosphorus acids.

Gobinda Chandra Behera

Dr Gobinda Chandra Behera is an Assistant Professor of Chemistry at M.P.C. Autonomous College, Baripada, Odisha, India, since 2018. His research interests include heterogeneous catalysis, materials chemistry, and the development of vanadium phosphate materials for liquid-phase organic transformations. He previously served as a Lecturer at Kendrapara Autonomous College (2016–2018) and N.C. Autonomous College, Jajpur (2014–2016). Dr Behera earned his PhD from CSIR–IMMT, Bhubaneswar, under Dr Kulamani Parida, and was a visiting research scholar at Cardiff University, UK. He has published 15 peer-reviewed research articles in international journals.

Sustainability spotlight

The intricate synthesis, hierarchical structure, and multifaceted applications of titanium phosphonates underscore their pivotal role in addressing global challenges across various scientific and industrial domains. By providing a comprehensive review, this article sheds light on the tunable properties of porous titanium phosphonates, which have significant implications for advancing sustainable technologies in industry, innovation and infrastructure. Their applications in catalysis, energy storage, and environmental remediation offer promising avenues for reducing environmental impact, enhancing energy efficiency, and promoting green chemistry practices as well as sustainable, inclusive economic growth. By bridging fundamental insights with practical applications, this work inspires interdisciplinary collaboration and sets a foundation for future breakthroughs that benefit society and the environment with value-added partnerships for goals.

1. Introduction

Hierarchical porous organic–inorganic hybrid materials have experienced significant advancements in the last two decades, driven by the development of tunable structures that incorporate metal nodes and suitable linkers. These materials are tailored depending on the dimensions and functionality of targeted complexes.[1,2] Moreover, these materials achieve versatility through an impressive research platform that leverages their unique properties, including organic functionality and flexible inorganic scaffolds. Open framework structures targeting cavities within the complexes require the use of bulky ligands with aromatic rings or alkyl chain derivatives. The key concept of pore chemistry is to incorporate structural voids that induce distinctive features, which help in integrating the framework backbone of hybrid materials and facilitating mass transfer through the interface.[3]

The use of polydentate ligands, tailoring metal–ligand geometry, and incorporating guest molecules/templating agents has proven to be a successful strategy for designing hybrid porous solids.[4,5] Among these, metal complexes with organophosphorus acids[6] and their derivatives as O-donors (Scheme 1) stand out as paradigms in these hybrid network structures due to their diverse coordination modes and potential applications in catalysis,[7,8] sensing,[9,10] sorption,[11,12] metal extraction[13] and optoelectronics.[14] Unlike the widely explored carboxylate-based metal–organic frameworks (MOFs), phosphonate-based MOFs/clusters remain relatively underexplored. The rational design of phosphonate MOFs *via* an isoreticular approach has emerged as a key synthetic strategy to broaden the scope of organophosphate materials.[15,16] While carboxylate- and multicarboxylate-based frameworks have been extensively investigated, with structures ranging from zero-dimensional clusters to three-dimensional porous frameworks,[17] phosphonate-based frameworks offer inherent structural flexibility and enhanced stability. To further diversify hybrid materials and to unlock novel functionalities, other phosphorus- and sulphur-based linkers such as phosphonates, phosphinates, phosphates, and sulphonates have also been explored. These linkers can mimic the carboxylate's coordination ability, and thereby serve as pioneering building units for the assembly of advanced porous materials.[18]

Since the 18th century, traditional porous structures such as zeolites, mesoporous silica, and activated carbons have been well-known as porous materials. However, they often encounter limitations in applications due to their rigid structural framework and lack of atomic-level structural tunability.[19,20] This rigidity hinders optimal interaction with reactants or gases, thereby limiting practical applications in specific fields such as catalysis or adsorption.[21] Later, new molecular sieve materials were developed for the first time featuring interconnected octahedral and tetrahedral oxide polyhedra, and showing novel compositions with larger pores and new topologies.[22,23] Subsequently, the introduction of hetero atoms into these frameworks emerged as one of the successful strategies for the formation of hybrid materials. Microporous titanium silicates (TS-1, ETS; Engelhard Corporation Titanosilicate) are used as active base catalysts in the dehydration of tertbutyl alcohol or the dehydrogenation of alcohols.[24] Simultaneously, other titanium hybrids like crystalline mono[25] and di-hydrated titanium phosphates[26] were investigated with a detailed study of their catalytic, ion exchange and proton conduction behaviour. Upon disclosure, their crystal structures exhibited significant differences in structural arrangement, while the degree of hydration influenced both the structure and the extent of ion exchange properties in both compounds. With high stability towards hydrolysis, di-hydrated titanium phosphates show greater ion exchange capacity. Later in 1997, Bortun *et al.* further studied these compounds with newly identified crystalline fibrous titanium(IV) oxophosphates.[27] This extended work resulted in MIL-n (MIL; Materials of Institut Lavoisier) series of compounds synthesized in the presence of fluorine and/or amines or

Kulamani Parida

Prof. Kulamani Parida is a globally renowned scientist in Materials Science, Catalysis, and Nanotechnology. He currently serves as Director and Distinguished Professor at the Centre for Nanoscience and Nanotechnology, Siksha 'O' Anusandhan (Deemed to be University). His research focuses on advanced functional materials for applications in fine chemical synthesis, energy, and environmental remediation. He has published over 627 high-impact research and review articles, holds 30 national and international patents, and has authored more than 10 book chapters. Prof. Parida has a citation count of 34 686, an h-index of 102, and an i10-index of 450.

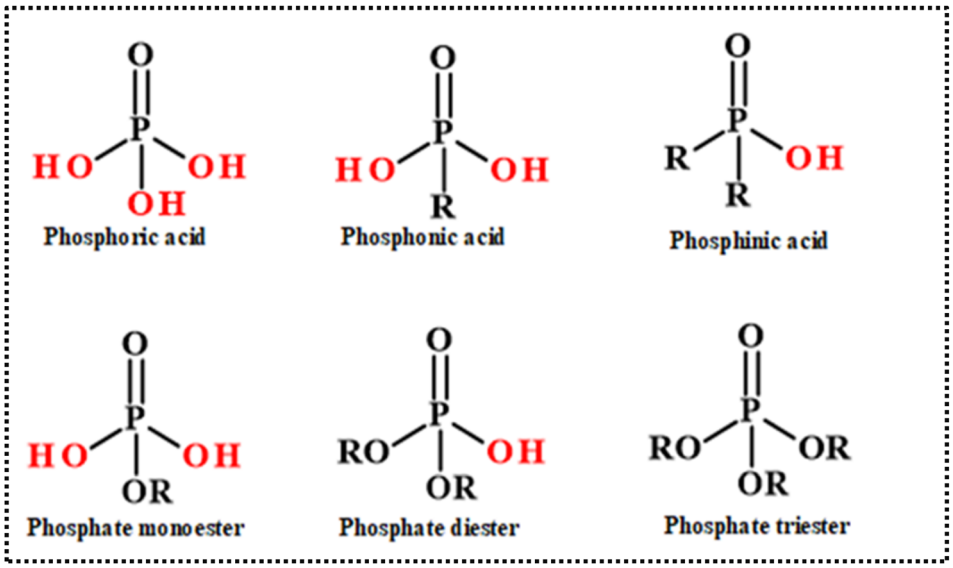

Scheme 1 Phosphorus-based acids with the maximum number of acidic protons (red) available.

surfactants. For example, $Ti_2(PO_4)_2F_4 \cdot (N_2C_2H_{10})$ (MIL-6_2) and $Ti_2(PO_4)_2F_4 \cdot (N_2C_3H_{12}) \cdot H_2O$ (MIL-6_3) consist of TiO_4F_2 octahedra connected by PO_4 tetrahedra with the interlayer space occupied by diammonium, bonded strongly with terminal fluorine atoms *via* hydrogen bonding.[28] It was observed that the charged templates are not a good option for developing these materials as the removal of organic groups leads to structural collapse. So, to avoid this difficulty, Alberti and Clearfield *et al.* proposed synthesis methods without using templates, and, thus, they started using diphosphonic acid instead of phosphoric acids, resulting into nonporous compounds like MIL-22 and MIL-25*n* ($n = 2,3$)[25,29](Fig. 1a–c).

As porous materials are quintessential in most scientific and technical fields, with useful applications ranging from catalysis,[30] separation,[31] energy storage,[32] and biomedical applications,[33] developing zeolite-type porous structures using various organic linkers has gained attention over the past two decades. In 2006, the first porous titanium(IV) MOF was fabricated by Serre *et al.* using *N*,*N*′-piperazinebismethylenephosphonate (O_3P-CH_2-NC_4H_8N-CH_2-PO_3), designated as MIL-91 ($Ti^{iv}O(H_2$-L)$\cdot nH_2O$).[34] Structural analysis revealed, as shown in Fig. 1d, a tancoite architecture featuring a framework of TiO_6 octahedral units surrounded by HPO_3C moieties, forming a channel-like structure (4 Å), with a reported surface area of approximately 500 $m^2\ g^{-1}$. The study demonstrated that organic linkers enhance tunability, which in turn enables the tailoring of organic–inorganic hybrid materials or clusters composed of metal ions bridged by organic linkers—introducing modularity to porous materials. Additionally, these phosphonate-based compounds exhibited well-defined control over intriguing structural characteristics to a greater extent and became highly sought-after in the field of porous materials.

The growing number of zeolite-like porous structures featuring phosphonates has received significant attention over the past two decades. While these materials address stability issues, they still encounter the challenging problem of nonporous, layered, and unpredictable structures due to extensive metal–oxygen binding through all three accessible oxygen atoms.[38] Thus, the challenge lies in synthesising phosphonate MOFs/clusters with imbued porosity. According to HSAB theory, phosphonate groups exhibit a strong affinity for hard metal ions such as Ti(IV), leading to thermally and chemically robust Ti(IV) phosphonates with hierarchical porous framework structures.[39] Additionally, the association of tetravalent Ti(IV) with phosphonate results in Ti(IV)–O–P bonds, providing high chemical stability even under extreme conditions of pH ≤ 1.[37] While this stability is beneficial for metal recovery and separation processes, it also limits control over reaction conditions due to inherent stability. On the other hand, phosphonates, $[RPO_3]^{2-}$ and their related ligands derived from phosphonic acids are particularly significant due to the presence of the P–C bond, which enhances stability and prevents hydrolysis, along with the +5 oxidation state of phosphorus (Scheme 1). Furthermore, the available P–O bonds allow oxygen to coordinate with metal ions, increasing the specificity of the complex through its multidentate behaviour, thereby enabling variations in the coordination environment of titanium phosphonates (TPs).[38]

-*R*, as an alkyl or aryl group, contributes to the orientation of the complexes in space and their electronic behaviour largely affects the intermolecular interactions, such as widely studied hydrogen bonds, pi–pi interactions, *etc.* Apart from this, many discrete units reported to date, such as titanium oxo clusters (TOCs), with diverse nuclearity show the highly oxophillic nature of the titanium metal ion.[40] Generally, titanium oxo core-based clusters are developed from a metal ion solution of $Ti(OR)_4$ in the presence of carboxylate/phosphate/phosphonate ligands, with control over parameters like reaction time, pressure, presence of water, reaction conditions like an inert atmosphere, *etc.* Various types of clusters with different Ti_xO_y cores are presented in Scheme 2 which shows the rich structural

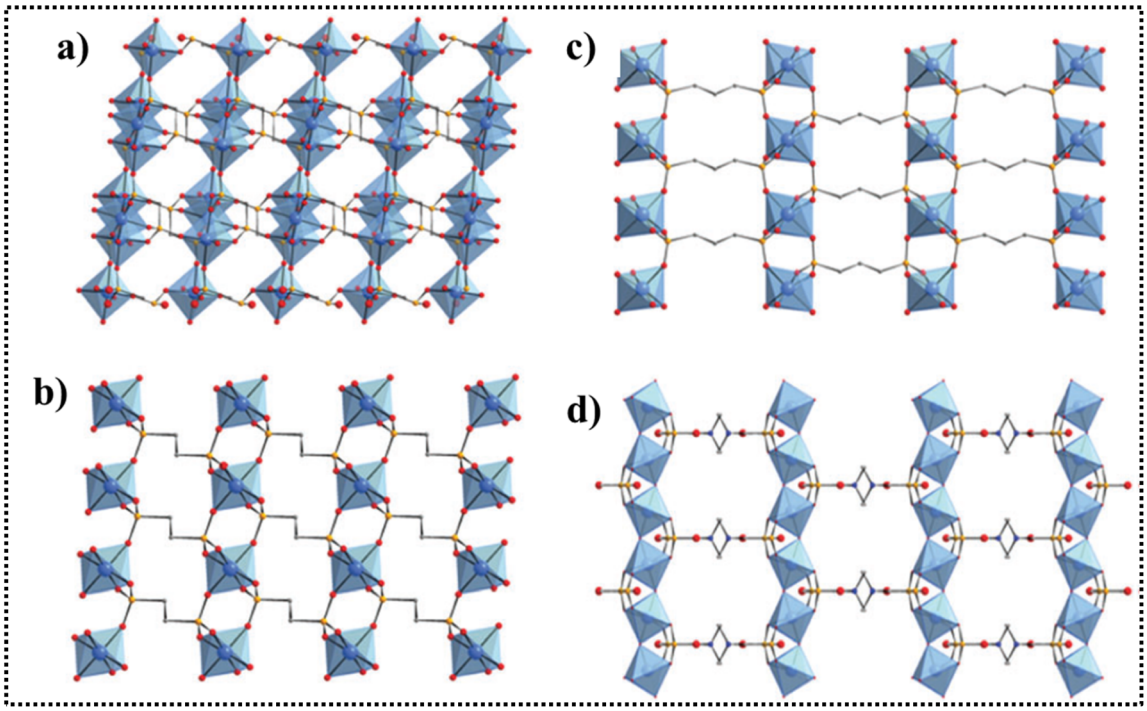

Fig. 1 Crystalline structures based on diphosphonate linkers: (a) MIL-22,[35] (b) MIL-25$_2$,[36] (c) MIL-25$_3$ (ref. 36) and (d) MIL-91(Ti)[34,37] color code: Ti, blue; O, red; C, grey; P, orange; N, dark blue. H-atoms of C-atoms were omitted for clarity. Adapted with permission from ref. 37. Copyright of The Royal Society of Chemistry, 2017.

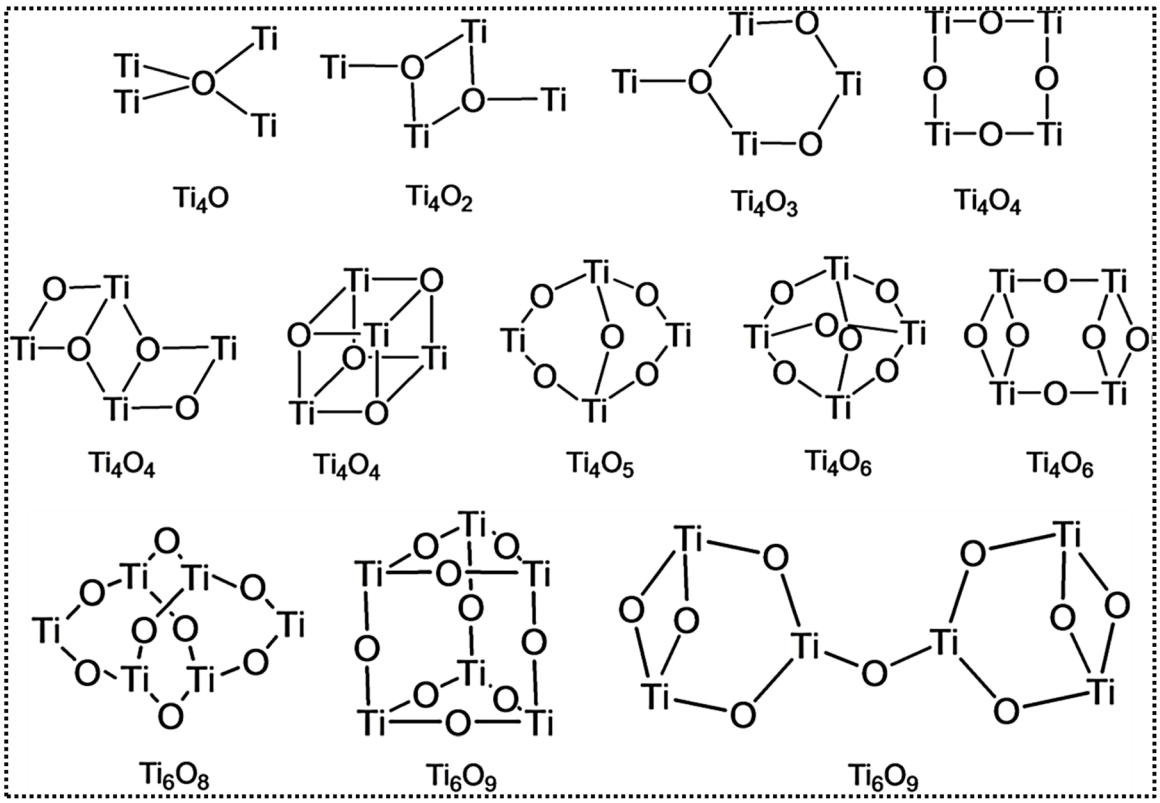

Scheme 2 Schematic core structures of various titanium oxo clusters.[41]

Table 1 Summary of the porous titanium phosphonates presented in this review[a]

Sl no.	HPTPs	Precursors	Morphology/type of structure	Crystallinity	Pore size/ peak maxima (nm)	Surface area $m^2\ g^{-1}$	Year	Ref.	Application
1		Arylphosphonic acid($ArPO_3H_2$) $Ti(OiPr)_2X_2$	Cluster	Crystalline	—	—	2018	51	Study of solubility and thermal stability
	1–5,7a	Ar=Ph(1), 1-Nap(2), 4-MeOPh(3), 4-FPh(4), 4-ClPh(5),4-BrPh(7) X = OiPr, Solv = THF(for 1 and 2) *i*PrOH(for 3–5, 7a) H_2O	Ti_4P_3 type	Crystalline					
	6,7b	4-BrBn(6) 4-BrBn(7b) X = OiPr H_2O	Ti_7P_6 type	Crystalline					
	8	Ar=Ph X = acac	Cage type	Crystalline					
2	1–5,7	*tert*-Butylphosphonic acid(*t*BPA) Titanium(IV) ethoxide Toluene-ethanol	Cluster	Partial crystalline	2–50, >50	—	2020	52	Controlling the hydrolysis conditions of complex structured oxide materials synthesis
3	6	*tert*-Butylphosphonic acid(*t*BPA) Titanium(IV)(diisopropoxide)bis(2,4-pentadionate) Acetone							
4	HM-TiPPh	1-Hydroxyethylidene-1,1-diphosphonic acid (HEDP) $TiCl_4$	Nanosphere	Amorphous	3–30	448	2018	53	Photocatalysis; H_2 evolution
5	PS-Ti-DEPP PS-Ti-DEBP PP-Ti-DEOP	Titanium tetraacetate ($Ti(OAc)_4$) Polypropylene (PP) Polystyrene (PS) Diethyl octylphosphonate (DEOP) Diethyl benzylphosphonate (DEBP) Diethyl phenylphosphonate (DEPP)	Fillers with a platelet-like structure	Amorphous	—	—	2023	54	Impact of solvent on morphology
6	HTiP-7	Benzene-1,3,5-triphosphonic acid (BTPA) Titanium(IV) isopropoxide	Nanosphere	Crystalline	1.4, 3.0, 4.8	255	2013	55	Optoelectronic
7	TOP	Tetrabutyl titanate, β-cyclodextrin (β-CD: $(C_6H_{10}O_5)_7$)	Reverse opal	Amorphous	400	23	2008	56	Photocatalysis; organic pollutant degradation
	TOPβ	1-Hydroxy ethylidene-1,1-diphosphonic acid (HEDP: H_2PO_3–$C(OH)(CH_3)$-PO_3H_2)				25			Heavy metal adsorption
8	TPPhA-Ti	Tetrakis-1,3,5,7-(4-phosphonate phenyl) Adamantane $Ti\{OCH(CH_3)_2\}_4$	Layered structures and film-like folded structures nanosphere	para crystalline	1.3–3.8, 180–300	557	2006	57	Structural study
9	PMTP-2	1-Hydroxy ethylidene-1,1-diphosphonic acid (HEDP) $TiCl_4$	Monolith	Crystalline	2.4	1034	2010	58	Ion exchange
10	H8L-Ti-MOF	1,1,2,2-Tetraphenylethylene (TPE)-phosphonate ester $Ti[OCH(CH_3)_2]_4$ $TiCl_4$	Nanosphere	Crystalline	1.2, 8.81	382	2021	9	Sensing, energy storage device

Table 1 (*Contd.*)

Sl no.	HPTPs	Precursors	Morphology/type of structure	Crystallinity	Pore size/ peak maxima (nm)	Surface area $m^2\ g^{-1}$	Year	Ref.	Application
11	PMTP-1	Ethylene diamine tetra(methylene phosphonic acid) (EDTMPS)	1D channel	Crystalline	2.8	1066	2010	59	Photocatalysis and metal ion adsorption
12	Ti–X (X = HE,BH,HP, PA,DT,PB)	Tetrabutyl titanate ($Ti(OC_4H_9)_4$)	Macro channels	Amorphous	100–2000		2017	60	Ammonia adsorption
	Ti–HE	1-Hydroxy ethylidene-1,1-diphosphonic acid (HEDP)				102			
	Ti–BH	bis(hexamethylene triamine penta(methylene phosphonic acid) (BHMTPMPA)				115			
	Ti–HP	2-Hydroxyphosphonocarboxylic acid (HPAA)				401			
	Ti–PA	Polyamino polyether methylene phosphonate (PAPEMP)				9			
	Ti-DT	Diethylene triamine penta (methylenephosphonic Acid) (DTPMPA)				85			
	Ti–PB	2-Phosphonobutane-1,2,4-tricarboxylic acid (PBTCA) tetrabutyl titanate				3			
13	TPPH	1-Hydroxyethylidene-1,1-diphosphonic acid (HEDP) tetrabutyltitanate ($Ti(OC_4H_9)_4$) P123 F127	Channels	Amorphous	2–3, 800–1200	511	2010	61	Metal ion adsorption/ CO_2 adsorption
14	CuO-dispersed titanium phosphonate	Ethylene diamine tetra(methylene phosphonic acid) $TiCl_4$ CuO	Hexagonal channels	Partially crystalline	~2.2	606	2010	62	Catalytic application & adsorption
15	TiPNW	Etidronic acid (EA) Titanium isopropoxide	Nanowire	Amorphous	~2	160	2020	63	Photocatalysis
16	Ti-AST	Alendronate sodium trihydrate (AST) $TiCl_4$	1D channel	Amorphous	2.4	540	2014	64	Acid–base bifunctional heterogeneous catalysis in CO_2 conversion
17	Titanium phosphonate hybrids	Tetrabutylorthotitanate ($Ti(OBu)_4$)		Partly crystalline			2022	65	Tuned sorption behaviour, solvent separation
	TiO_2–C3	1,3-Propyldiphosphonic acid (PrDPA)	Less layered		Mesoporous	379			
	TiO_2–C8	1,8-Octyldiphosphonic acid (ODPA)	Layered			329			
	TiO_2–Ph	1,4-Phenyldiphosphonic acid (PhDPA)	Layered			334			

[a] NB: the numbers mentioned in Sl no. 1, 2, and 3 are the cluster numbers for the compounds as shown in Scheme 3.

chemistry of oxo compounds with μ_2, μ_3, and μ_4 bridged oxo groups.[41,42] Although its preferred coordination number is 6 it also exhibits 5- or rarely 4- and 7-coordinated structures; as a result, more than 500 polynuclear homometallic Ti(IV) compounds have been analysed by Single Crystal XRD structure analysis. In addition to this, in the coordination environment, apart from neutral ligands, anionic ligands play a dual role in these compounds, often stabilising the structure by balancing the residual charge of the oxo core Ti_xO_y as $y < 2\times$, while simultaneously satisfying the coordination sphere of the metal ion.[41]

The high reactivity of Ti(IV) makes the formation of crystalline coordination polymers and MOFs particularly challenging. However, these materials hold significant promise for photocatalytic and optoelectronic applications. Among various tetravalent phosphonates reported, titanium(IV) is an impressive candidate due to its low cost, and redox, semiconducting,[43,44] and photocatalytic properties.[45] Titanium phosphonates have been widely reported as discrete units, clusters, 1D, 2D and 3D coordination polymers and MOFs. This precision arises from the ability to alter pore size, shape, and functional groups by selecting specific metal nodes and linkers as well as modifying the resulting frameworks post-synthetically to achieve the desired properties. This unique feature bestows MOFs/hybrid porous materials with several advantages, such as high surface area, tunable porosity, and specific interaction sites, enabling a wide range of potential applications. Hierarchical porous titanium phosphonates (HPTPs), characterised by multiple pore scales (micropores, mesopores, and macropores), overcome diffusion limitations typically observed in conventional microporous MOFs or single-sized porous materials by facilitating enhanced mass transport.[46] Interconnected porous structures in hierarchical architectures enhance the practical utility of hybrid materials, making them ideal for applications that require rapid molecular diffusion, such as catalysis of large-molecule reactions, gas storage, air filtration, wastewater treatment, *etc*.[1] These properties can be further modified, incorporating new functional groups (–OH, $–NH_2$, and –COOH) into the organic linkers, aiding precise control over electronic structures at the molecular level. In some cases, mixed linkers offer additional advantages, by introducing multiple characteristics into the hybrid materials, such as tunable pore size, increased surface area, and enhanced electronic behaviour, complemented by more accessible active sites. Moreover, these materials influence the adsorption behaviour due to the enhanced interactions occurring with the guest molecules during the process. The introduction of hydrophilic/hydrophobic groups in linkers is particularly beneficial for solvent separation applications.[5] An overview of the porous titanium phosphonates discussed in this review is provided in Table 1.

The limited number of reviews on hierarchical porous materials of metal phosphonates or phosphate underscores the need for a comprehensive compilation of titanium phosphonates, which are yet to be reviewed, to provide insights into this emerging field of research. While our group has extensively studied MOF-based photocatalytic applications[47–50] and has contributed numerous review articles on this topic, many remarkable porous hybrid materials remain unexplored and require a broader, more comprehensive analysis. This review aims to explore recent advancements in titanium phosphonate MOFs, clusters and hybrid complexes, focusing on their coordination environment and hierarchical porosity. Additionally, it emphasises synthetic strategies to overcome the unpredictable behaviour of the Ti(IV) metal ion in forming targeted structures, along with an analysis of structure–property relationships.

2. Rational fabrication of porous titanium(IV) phosphonates

Various synthetic strategies have been developed to produce porous titanium(IV) phosphonates (PTPs) based on different precursors as linkers. Template-assisted synthesis is the most versatile and convenient approach to generate hybrid porous structures with significant performance in photocatalytic hydrogen evolution. HPTPs are synthesized *via* a facile hydrothermal process using a polyelectrolyte–surfactant system, for example, the cationic surfactant cetyltrimethylammonium bromide (CTAB) and an anionic polymer like poly(acrylic acid) (PAA). These components facilitate electrostatic interactions, enabling the co-assembly of precursors into well-defined hierarchical mesoporous structures.[63] Nanostructured HPTPs are difficult to synthesise using the conventional hydrothermal method. Instead, a stirring hydrothermal technique is employed, in which mechanical force plays a crucial role in structural orientation along the axial direction, facilitating mass transfer and leading to the formation of nanowires. Titanium phosphonate adsorbent materials are synthesized from tetrabutyl titanate and various organophosphonic acids including (1-hydroxy ethylidene-1,1-phosphonic acid (HEDP), bis(hexamethylene triamine penta(methylene phosphonic acid)) (BHMTPMPA), 2-hydroxyphosphonocarboxylic acid (HPAA), 2-phosphonobutane-1,2,4-tricarboxylic acid (PBTCA), polyamino polyether methylene phosphonate (PAPEMP), and diethylenetriamine penta(methylene phosphonic acid) (DTPMPA) *via* a hydrothermal route. After the complete hydrolysis of titanium alkoxide, the homogeneous mixture is transferred to an autoclave and heated at 80 °C for 24 h, yielding HPTPs.[60]

Hybrid porous titania phosphonate sorption materials are also synthesized following the above method with post synthetic treatment using bridged diphosphonic acids (DPAs) and $Ti(OBu)_4$ in a water–ethanol mixture at 30 °C. The successful incorporation of DPAs into the titania matrix is observed with quantitative yield of the hybrid materials based on the Ti/2P ratio using different types of filtration tools to separate them.[65] A surfactant-assisted hydrothermal method is used, where Brij 56 acts as a structure-directing agent along with Alendronate Sodium Trihydrate (AST) and $TiCl_4$ to prepare mesoporous Ti-AST. Controlled hydrolysis and condensation conditions are maintained at a P/Ti molar ratio of 5 : 3 and pH ~4.0, adjusted using ammonia and hydrochloric acid, followed by stirring for 2 h. Thereafter, the solution mixture is sealed in

a Teflon-lined autoclave and aged at 120 °C for 48 hours under autogenous pressure.[64]

In situ synthesis of titanium phosphonate/polymer composites *via* a nonhydrolytic solgel route is another remarkable process that highlights the importance of solvent in the growth and morphology of nanocomposites. Unlike the traditional water-based hydrolytic sol–gel processes, this method employs organic solvents to control polycondensation reactions, leading to materials with higher hydrothermal stability and controlled porosity. A viscous polymer medium, polypropylene (PP) or polystyrene (PS), was used to incorporate layered metal phosphonate fillers, which were synthesized in a Haake® internal mixer, achieving 10 wt% titanium phosphonate in the final composite with titanium oxide precursor $Ti(OAc)_4$. The molten polymer, fabricated by modulation of the aspect ratio confirms the presence of P–O–Ti bonds.[54] Similarly by maintaining a constant molar ratio of Ti and BTPA (benzene-1,3,5-triphosphonic acid) without altering the reaction time (24 h), several HPTP complexes (HTiP-7A, HTiP-7B, HTiP-7C and HTiP-7D) were developed by varying the pH of the synthetic gel and hydrothermal temperature. The synthetic gel was prepared by the slow addition of phosphonic acid solution to the alcoholic titanium-isopropoxide solution, followed by overnight stirring before transferring it into an autoclave for thermal agitation at 453 K. The mixture was then centrifuged at 5000 rpm and suspended in dry ethanol to obtain the desired nanoparticles. This self-assembly process yields the product without the use of any surfactant or templating agent.[55]

Macroporous titanium phosphonate materials were also synthesised *via* the hydrothermal method, using the inverse opal method with a microwave-treated PS sphere as a hard template. This technique uses colloidal crystals (often silica spheres or polystyrene spheres) as a sacrificial template for the production of extremely ordered macroporous structures upon removal of the template. HEDP (1-hydroxyethylidene-1,1-diphosphonic acid) and tetrabutyl titanate were used as precursors to form a homogenous solution, which was statically agitated at 60 °C, followed by extraction of spheres with a THF/acetone(1 : 1 of v/v) mixture solution for 48 h.[56]

The dendritic tetrakis-1,3,5,7-(4-phosphonatophenyl) adamantane precursor, along with titanium(IV) isopropoxide, is used to overcome the challenges of close pillar disposition and limited control over pore size in the organic–inorganic hybrid HPTPs. Instead of ditopic building blocks, tetratopic ligands with extended tetrahedral symmetry, are used *via* a non-hydrolytic condensation pathway producing insoluble materials with a Ti/P ratio of ~1. HPTPs exhibited different morphologies depending on the solvent used in the condensation reactions, for example, from layered compounds to hollow nanospheres.[57]

Evaporation-Induced Self-Assembly (EISA) utilizes a soft template approach, where surfactants spontaneously diffuse towards the vapor phase and utilize solvent evaporation to create mesoporous structures. This differs from the mild solvent evaporation technique, in which the evaporation of solvent is slow and controlled in order to deposit precursors, which is known to yield denser, less porous materials compared to EISA. In the synthesis of HPTPs, self-assembly strategies such

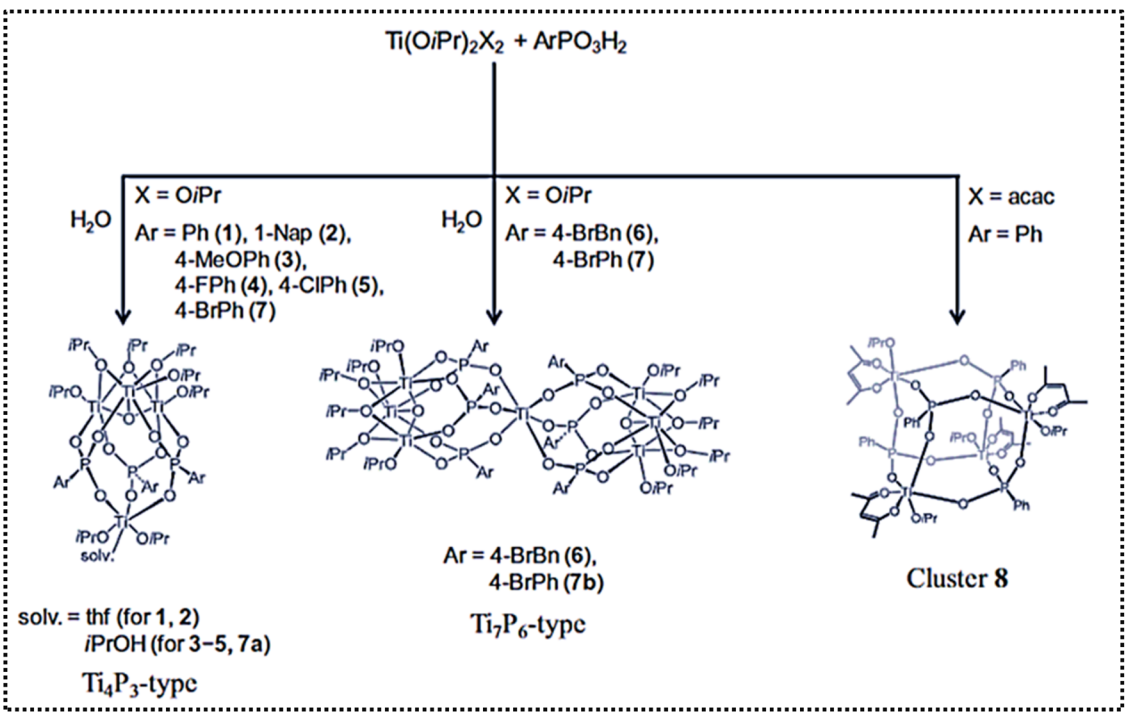

Scheme 3 Synthesis of clusters (**1–8**), illustrating the stepwise formation and structural variations in polyhedral metal clusters Ti_4P_3,Ti_7P_6-type and cluster **8**. Adapted with permission from ref. 51. Copyright of The Elsevier, 2018.[51]

as autoclaving followed by a slow evaporation process are often employed. Additionally, EISA can be functionalised by $ClSO_3H$ treatment due to its strong catalytic behaviour and ion exchange capability. In this process, HEDP and $TiCl_4$ are used in combination with the non-ionic surfactant Brij 56. After autoclaving, white gel blocks are produced, and upon surfactant removal during extraction, a yellowish hue with hard texture is developed. However, the shape of the monoliths remains well preserved, retaining periodic mesoporosity.[58] In some instances, an unprecedented polydentate claw molecule, sodium salt of ethylenediamine tetra(methylene phosphonic acid) (EDTMPS), is also used as a coupling agent. These organic–inorganic hybrids proved to be more tunable compared to purely inorganic porous materials.[59] In a similar process EDTMPS and $TiCl_4$ (P/Ti molar ratio: 4/3) are placed in a reactor kept in a cryosel bath to slow down the hydrolysis process. The pH value is maintained at 4.0 throughout the reaction using ammonia and HCl solution, ultimately yielding HPTPs with well-defined structures.[62]

A mild solvent evaporation strategy was employed using tetrabutyl titanate and HEDP as an organophosphorus coupling molecule to yield HPTPs. In this process, triblock copolymers F127 and P123 acted as structure-directing agents. The reaction mixture was stirred for 24 h and then transferred into Petri dishes to allow ethanol evaporation under controlled relative humidity at 40 °C in the air for 2 days. The surfactant was subsequently removed by ethanol extraction over 96 h.[61] Beyond MOFs, hybrid networks, for example, clusters (**1–7**) were developed by using titanium tetraisopropoxide ($Ti(OiPr)_4$) and various aryl phosphonic acids, both in the presence and absence of solvent. Additionally, titanium bis(acetylacetonate) diisipropoxide [$Ti(acac)_2(OiPr)_2$] was used to develop cluster **8** under solvent free conditions, as depicted in Scheme 3.[51] Arylphosphonic acids ($ArPO_3H_2$) were prepared *via* the alcoholysis of phosphonate esters, which were synthesized *via* the Arbuzov reaction.[66,67]

High porosity depends on both the denticity of the ligand and its geometric pattern, which determine how it coordinates with the metal ion in a MOF structure. For example, tri and tetratopic ligands with rigid structures yield porous frameworks. Similarly, a nanoporous Ti-phosphonate MOF was reported using a novel tetradentate phosphonate ligand and $TiCl_4$ as precursors, synthesized *via* a hydrothermal method at 180 °C for 48 h.[9]

3. Structure and morphology

Owing to variable oxidation states, the unpredictable reactivity of the Ti(IV) metal centre is often associated with the intriguing coordination modes. However, the challenging synthesis process results in poor control over the structure and properties of hybrid materials, such as Ti-based oxo-clusters, coordination polymers, and MOFs. Despite these challenges, titanium complexes continue to fascinate the research community due to their promising photocatalysis and optoelectronic properties. While divalent and trivalent transition metal ions have been extensively studied, yielding thousands of framework structures, their stability, remains a significant limitation. These frameworks are often susceptible to hydrolysis or exhibit unprecedented porosity, with less ordered structures, limiting their practical applications. To address these challenges, tetravalent frameworks have been explored. However, their high reactivity often leads to precipitation or poorly crystallised materials. In this context, Zr(IV) is an exception, as UiO-66 has proven to be one of the most robust materials. It is not only tunable but also facilitates the successful synthesis of hybrid materials and MOFs through an isoreticular approach. Similarly, titanium as a tetravalent cation, has been utilised to produce MOFs, oxo clusters, and organic–inorganic hybrid matrices, although with lower crystallinity.

Titanium phosphonates (TPs) exhibit diverse morphologies such as platelets, nanowires, nanospheres, channels, layers, monoliths, *etc.* (Fig. 6) each contributing uniquely to hierarchical porosity, which is crucial for applications in catalysis, adsorption, energy storage, and separation. Platelet-like TPs feature layered plate-like structures with tunable interlayer spacing, where microporosity arises from interlayer gaps, which contribute to a high surface area and are also responsible for the interaction of small molecules. Other types of porosity like mesoporosity from platelet aggregation, and macroporosity from stacking voids are observed, largely depending on the synthetic process followed. These properties make them well-suited for catalysis, adsorption, and composite materials. Nanowire TPs, characterized by their one-dimensional, high-aspect-ratio structures, exhibit microporosity due to surface defects, mesoporosity from interwire gaps, and macroporosity resulting from assembly of subunits. These materials excel in energy storage, catalysis, and adsorption applications. Nanosphere TPs, on the other hand, form spherical architectures that can be solid or hollow, with their size and porosity tunable through synthetic techniques. Their hierarchical porosity includes microporosity resulting from ligand selection, mesoporosity introduced by templating or etching, and macroporosity resulting from interparticle voids, making them effective in drug delivery, catalysis, and energy storage. The hierarchical porous network is built by the arrangement of nanospheres on the bulk scale and can be tailored under controlled conditions for various potential applications.

Channel-based TPs form interconnected porous networks in 1D, 2D, or 3D frameworks, where microporosity originates from the intrinsic framework, mesoporosity from templating methods, and macroporosity from hard templating techniques. Their highly organized channels make them especially suitable for ion exchange, catalysis, adsorption and separation processes. Similarly, layered TPs consist of alternate inorganic Ti–O and organic–P layers forming lamellar structures. These TP layers are staked through non-covalent interactions like van der Waals forces or hydrogen bonding. Interlayer distances can be tailored using various phosphonic acid linkers and intercalating guest molecules. Furthermore, functionalisation in the organic linkers affects the layer structure, porosity and functionality. A self-supporting, robust, interconnected, continuous architecture forms TP monoliths which on integration with a well tuned pore hierarchy makes them highly effective for

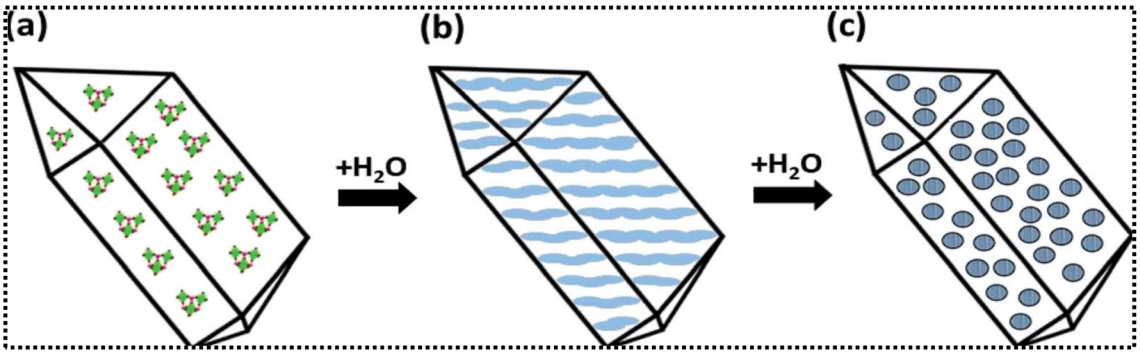

Fig. 2 Transformation of an (oxo) alkoxide crystal (a) to a crystalline anatase core (b) results in the disordering of the amorphous phase (c) upon hydrolysis. Adapted with permission from ref. 52. Copyright of Royal Society of Chemistry, 2020.

applications in separation and ion exchange processes. Unlike other forms of TPs, they produce a single framework which enhances structural integrity and prevents self-aggregation, an issue observed in other morphologies. The various morphological forms discussed in this review are elaborated categorically as follows.

Cluster titanium phosphonates (TPs) form a unique subclass of these materials, characterized by discrete Ti–O–P clusters that function as well-defined nanoscale building blocks. These clusters can be integrated into larger frameworks, contributing to hierarchical porosity by creating micropores within the clusters and meso to macropores through their arrangement pattern in the bulk material. However, the full extent of cluster-based porosity remains relatively unexplored, especially concerning the impact of aggregation and surface modifications influencing pore connectivity and accessibility. Gunji and co-workers reported eight single crystal clusters featuring three distinct core structures: Ti_4P_3, Ti_7P_6, and a distorted cubic framework, all exclusively composed of Ti–O–P bonds as shown in Scheme 3. Clusters **1** and **3** are crystallised in the triclinic $P\bar{1}$ space group, cluster **7** adopted the trigonal $P\bar{3}$ space group, while the remaining clusters crystallised in a monoclinic system.[51] In Ti_4P_3, four titanium metal centres exhibit octahedral geometry, each coordinated by five terminal and three bridging isopropoxy groups. Moreover, the presence of solvent adducts contributes to the stability of the coordination environment. The Ti_7P_6-type cluster consists of two $[Ti_3(\mu_3\text{-}O)(OiPr)_3(\mu\text{-}OiPr)_3](Ti_3O)$ units, six aryl groups (4-bromobenzyl for cluster **6** and 4-bromophenyl for cluster **7b**) and a central titanium atom aligned along the C_2-symmetry axis. Notably, cluster **7** is a cocrystal comprising two Ti_4P_3 clusters and one Ti_7P_6 type cluster. In contrast, cage-type cluster 8 is a distorted-cubic framework formed by four titanium atoms, four phenyl phosphonate groups and four isopropoxy groups, all chelated by acetylacetonato groups. Each metal centre is coordinated by one chelating *acac* group, one isopropoxy group and three bridging phenyl phosphonato groups connecting to other metal centres. This coordination environment highlights the influence of chelating groups and the steric hindrance introduced by para-substituents, which significantly affect the core structure of the clusters, as observed in both Ti_4P_3 and Ti_7P_6 type clusters. Similarly, Kessler and co-workers reported seven oxo alkoxide multinuclear clusters synthesized using solvothermal or reflux condensation methods, labelled 1 to 7, showing phosphonate ligand's bidentate and tridentate nature in coordinating metal ions. These clusters exhibit varying nuclearities, such as tetranuclear (**2**, **3**, **4** and **6**), pentanuclear (**1** and **7**), and hexanuclear (**5**) structures. The clusters are stabilized by various oxocores with suitable μ2, μ3 and μ4 bridges contributed by phosphonate and alkoxide (ethoxide/isopropoxide) groups.[52] Bridging the titanium atom with μ_2, μ_3, and μ_4 oxo groups plays a crucial role by terminating the coordination sites, making the core more compact and condensed, thus enhancing the stability of the complexes. Clusters **1**, **3**, **4** and **6** are crystallised in the monoclinic system while clusters **2**, **5** and **7** adopt the triclinic crystal system. The pentanuclear oxo core cluster **1** consists of Ti_3O units connected by μ_3-O bridges, with phosphonate ligands coordinating to the metal centre in both tridentate and bidentate fashions. These examples demonstrate that incorporating multiple oxo bridges significantly influences the structural features of titanium–oxo complexes as they affect the nuclearity, geometry and stability of the cluster. Notably, upon hydrolysis, these clusters undergo a topotactic transformation, contracting from crystalline materials to densified structures featuring a crystalline core and an amorphous outer shell, as depicted in Fig. 2.

The development of platelet like titanium phosphonate-based nanocomposites *via* a non-hydrolytic sol–gel process within a viscous polymer medium is influenced by both the choice of phosphonate precursors and the polymer matrices employed. Specifically, diethyl phosphonates serve as the precursors, while polypropylene (PP) and polystyrene (PS) are utilised as the polymer matrices.[54] The resulting nanocomposites exhibit distinct morphologies: in PP, fillers display amorphous platelet-like structures (less organised), whereas in PS, a layered (more organised) configuration is observed. The variation is attributed to the molecular mobility provided by the linker in DEBP/DEPP, which is associated with the PS matrix and facilitates π–π stacking interactions between aromatic groups. Such interactions promote better compatibility and

integration between the filler and polymer matrix, leading to more organised layered structures. In contrast, the PP matrix lacks such interactions, resulting in less organised structures. Layered titanium phosphonates in the PS matrix result in an interlayer spacing of about 13.2 Å, leading to improved filler dispersion and reduced aggregate formation. The presence of P–O–Ti bonds within the MOF is effectively confirmed by FTIR and 31P NMR spectroscopy. When DEBP is used as a phosphonate precursor, the resulting PS-Ti-DEBP fillers are smaller (500 nm in length and 85 nm in width) and exhibit uniform dispersion. In contrast, when DEPP is employed, larger PS-Ti-DEPP fillers are formed. The introduction of a flexible methylene (CH_2) group in the diethyl benzylphosphonate (DEBP) linker enhances molecular mobility within the polystyrene (PS) matrix. This increased flexibility facilitates more effective π–π stacking interactions among aromatic groups, leading to the formation of smaller, well-dispersed fillers. In contrast, the absence of the CH_2 group in diethyl phenylphosphonate (DEPP) results in reduced molecular mobility, contributing to the formation of larger aggregates within the PS matrix. This structural design prioritizes thermal stability and solubility over porosity.

The extensively condensed HM-TiPPh MOF, characterised by hierarchical porosity, and amorphous nature, demonstrates high efficiency in photocatalytic hydrogen evolution. Mesomorphous liquid-crystalline phases, composed of building units, formed by Ti(IV) metal centres and 1-hydroxyethylidene-1,1-diphosphonic acid (HEDP), are coassembled through an ionic self-assembly mechanism. These formations are further stabilised by interactions with the surfactant cetyltrimethylammonium bromide (CTAB) and an oppositely charged polyelectrolyte, poly(acrylic acid) (PAA).[53] Fig. 3(a–d) show nanospheres with interstitial pores (left) alongside a schematic illustration of the assembly process (right), which follows the dual template method to achieve hierarchical porosity. The compositional homogeneity enhances light absorption, facilitates charge separation, and increases active site accessibility while also reducing material wastage and mitigating the recombination of photogenerated electrons and holes through the strategic distribution of electron traps.

HTiP-7, another titanium phosphonate nanosphere, crystallises in the triclinic system, where titanium ions are interconnected with phosphonate ligands. The formation of P(O–Ti)$_3$ units occurs as each phosphonate group from the BTPA ligand coordinates with three titanium atoms.[55] As a result, a porous network emerges, integrating both micropores and mesopores with pore sizes centred around 1.4 nm, 3.0 nm, and 4.8 nm. Self-assembled nanoparticles with spherical morphology are facilitated by π–π stacking interactions between the aromatic rings of the BTPA ligands. The presence of mesopores, ranging from approximately 3.0 to 5.0 nm, subsequently helps in the adsorption of guest molecules. Macroporous titanium phosphonate materials (TOP), as reported by Yuan and co-workers, feature a three-dimensional ordered network synthesized using 1-hydroxyethylidene-1,1-diphosphonic acid (HEDP) as the phosphonate precursor.[56] After the removal of the PS spheres (template) a void network is created, which is subsequently filled with titanium phosphonate gel, leading to a highly ordered macroporous structure with pore sizes around 400 nm. The titanium phosphonate framework adopts a reverse opal pattern, where the voids left by the original template spheres remain interconnected, forming large cages with internal spaces that enhance light distribution and facilitate mass transfer throughout the material (Fig. 4). Efficient filling of the voids with titanium phosphonate gel was achieved due to the thin pore walls (~10–20 nm). In TOPβ (a β-cyclodextrin; β-CD derivative), the pore walls considerably thicken to around 200–400 nm, leading to a less ordered structure, with an increase in adsorption sites for metal ion uptake.

HEDP enhances the mechanical strength and ductility compared to purely inorganic phosphonate precursors, which are more commonly used and exhibit distinct structures as reported in the literature.[68–70] The well-ordered mesoporous framework, monolith PMTP-2, is an inorganic–organic hybrid with hexagonal symmetry, composed of a titanium phosphonate framework that incorporates HEDP. It has a pore size of approximately 2.4 nm, with a pore wall thickness of around 1.8 nm. This mesoporous structure, characterised by its unique composition, structural features, and potential for

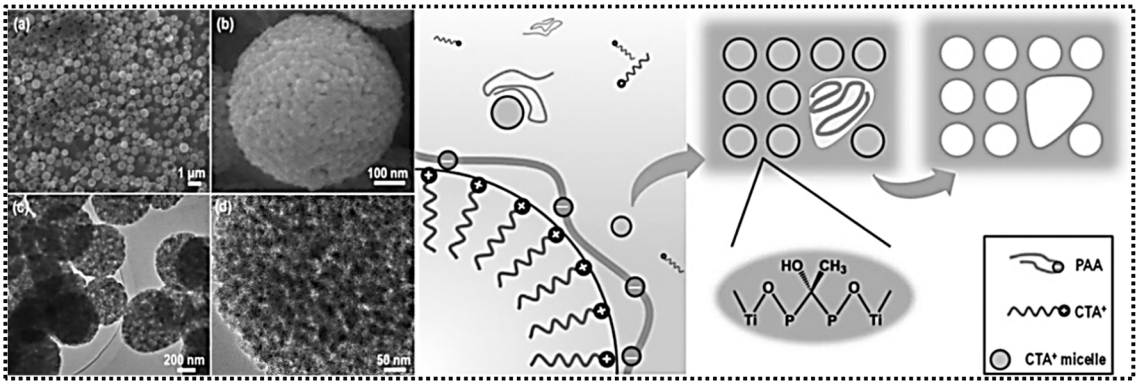

Fig. 3 (a) SEM image of high yield spheres of HM-TiPPh. (b) Higher resolution of nanospheres showing a rough surface. (c) TEM image showing contrasting interstitial pores. (d) Secondary mesopores with larger size. The dual template method used in the formation of hierarchically porous titanium phosphonates (right). Adapted with permission from ref. 53. Copyright of Wiley, 2018.

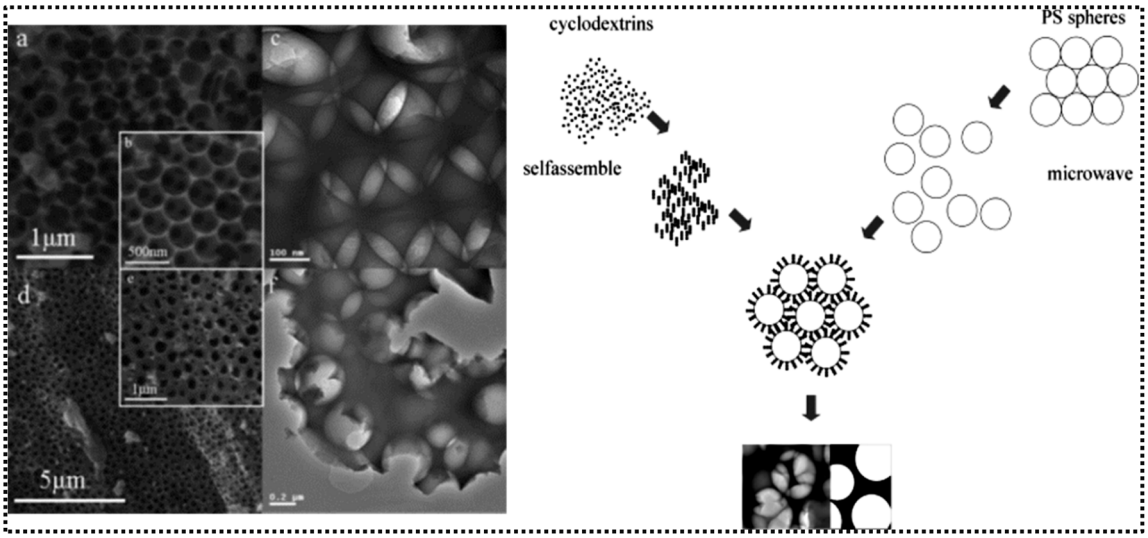

Fig. 4 (a and b) SEM and (c) TEM images of TOP; (d and e) SEM and (f) TEM images of TOPβ (left). Scheme of formation of TOPβ (right). Adapted with permission from ref. 56. Copyright of American Chemical Society, 2008.

functionalization, presents promising applications in ion exchange, catalysis, and as an electrolyte in fuel cells.[58] Yuan *et al.* developed another HPTP, a titanium organophosphonate hybrid framework, utilising structure-directing agents F127 and P123, along with a titanium precursor and HEDP, which acts as an organophosphorus coupling agent molecule.[61] The triblock copolymers function as templating agents and aid in the self-assembly process to form a one dimensional macro channel structure. The macroporous framework (800–1200 nm in diameter) integrates a mesophase (2–3 nm in diameter), facilitating gas and liquid transport, while enabling metal ion binding through coordination. This structural hierarchy enhances adsorption efficiency, contributing to improved porosity and functionality. A single broad diffraction peak in the low-angle region confirms the aggregation of titanium phosphonate nanoparticles, which fill the mesovoids along the macroporous channel wall. This structural arrangement plays a crucial role in forming an interconnected network that improves adsorption by increasing the surface area and accessibility for on-site reactions in HPTPs.

Dendritic tetraphosphonates, such as tetrakis-1,3,5,7-(4-phosphonate phenyl)adamantane (TPPhA), serve as tetrahedral organic building blocks that significantly impact structural organisation of the hybrid organic–inorganic framework.[57] The phosphonate groups (P–O) from the TPPhA units coordinate to titanium atoms in a bidentate manner, as confirmed by FT-IR and NMR spectroscopy, which indicate bonding between phosphonate oxygen atoms and titanium, while excluding interactions between the P=O group and titanium. This coordination follows a characteristic $P(O)O_2Ti_2O_2(O)P$ pattern,

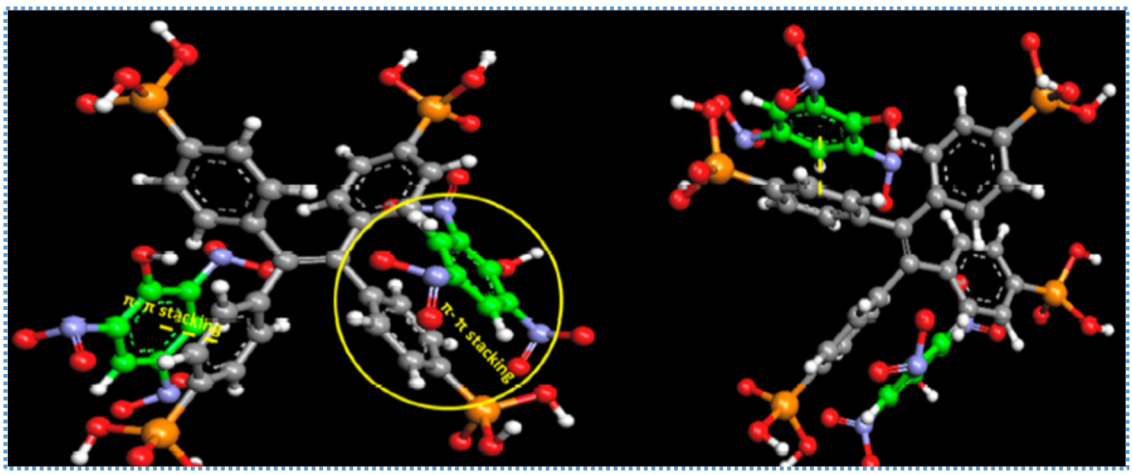

Fig. 5 pi–pi interaction between the targeted TNP and aromatic moieties of the H8L-Ti MOF as shown by the yellow circle. Adapted with permission from ref. 9. Copyright of American Chemical Society, 2021.

preventing close packing and promoting the hierarchical porous structure with both microporosity (13.5 Å) and mesoporosity (38 Å). The material primarily exhibits two primary morphologies: (i) a plate-like layered structure, where the plate exhibits a lamellar arrangement, and (ii) folded films, appearing as thin film-like structures that occasionally curl or roll at the edges. Additionally, by varying synthetic routes, hollow nanospheres (180–300 nm in diameter) composed of a titanium oxide-phosphonate mixture have been synthesized, highlighting the influence of solvent selection on the assembly process. This porous material possesses both amorphous and partially ordered (paracrystalline) characteristics, as indicated by broad peaks in X-ray diffraction patterns, signifying a disordered framework with localised periodicity in certain regions.

A novel nanoporous Ti-phosphonate MOF (H8L-Ti-MOF) has been synthesized using another tetradentate phosphonate ligand, 1,1,2,2-tetraphenylethylene (TPE)-phosphonate ester (H_8L). The tetratopic arms coordinate with titanium ions, leading to a monoclinic crystalline phase with high chemical and thermal stability and adopting a nanosphere morphology.[9] This three-dimensional crystalline structure exhibits hierarchical porosity, comprising micropores with a pore size of approximately 1.2 nm and mesopores with a pore size of about 8.81 nm, facilitating the accommodation of guest molecules, making the MOF suitable for sensing applications. Furthermore, the extensive π-conjugation in the ligand structure improves ion transport, thereby enhancing the material's performance as a supercapacitor by boosting conductivity and charge storage capabilities, as illustrated in Fig. 5.

The mesoporous titanium phosphonate material (PMTP-1) is synthesized using ethylenediamine tetra(methylene phosphonic acid) (EDTMP) ligands, which coordinate with titanium (Ti) centers to form a stable 1D channel framework.[59] The phosphonate groups serve as coupling molecules, providing both structural integrity and substantial functionality to the framework. EDTMPS can be protonated or alkylated by adding HCL or NaOH, respectively. Additionally, the organic bridge containing the ethylene diamine moiety plays a crucial role in influencing the physicochemical properties of the material. The presence of a hexagonal (*p6mm*) mesophase is confirmed by X-ray diffraction (XRD), which shows a primary peak corresponding to the (100) reflection, indicating well-defined mesoporosity. The average pore size is approximately 2.8 nm, with a pore wall thickness of 1.8 nm, enabling effective transport and interaction of guest molecules.

PMTP-1 exhibits a robust nature, as it is thermally stable up to 450 °C, and upon calcination above 550 °C, it converts into an amorphous titanium phosphate network, while partially preserving its mesoporosity. The material exhibits a one-dimensional (1-D) channel structure and its morphological versatility allows for the fabrication of various forms, such as monoliths, cubes, and powders, making it suitable for diverse applications. EDTMP also serves as a phosphonate precursor in mesoporous inorganic–organic hybrids (MTPs), which have been integrated as a support for CuO nanoparticles.[62] In addition to mesopores, irregular macrovoids (large voids or cavities) are dispersed throughout the microspheres, which are formed by the accumulation of titanium phosphonate nanoparticles. This structural arrangement forms hexagonal channels which enhance the surface area and promote diffusion, facilitating efficient mass transfer of reactants and products in catalytic reactions. The spherical morphology and uniform pore distribution with an average size of 2.2 nm, provide a large surface area-to-volume ratio, ensuring effective dispersion in catalytic systems. The titanium oxide framework, stabilised by P–O bonds, plays a crucial role in coordinating metal ions such as copper. Following calcination, the mesophase remains intact, allowing the incorporation of well-dispersed CuO nanoparticles (CuO-MTPs), further enhancing catalytic efficiency. Moreover, the material's excellent thermal stability is essential for high-

Table 2 Listing of Phosphonate precursors

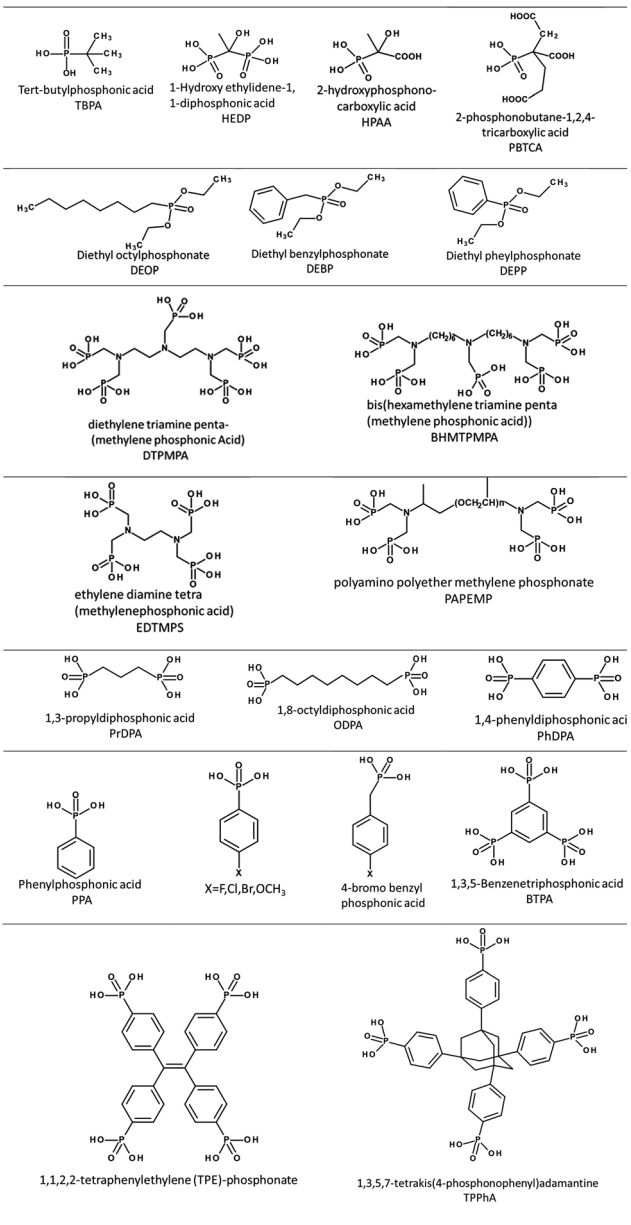

temperature catalytic applications, as it ensures structural integrity under extreme conditions. The high surface area and stability of this HPTP make it an effective support for catalytic processes, particularly by promoting the dispersion and stabilisation of CuO nanoparticles.

Titanium phosphonate adsorbent materials featuring a hierarchical porous structure have been reported, exhibiting macropores ranging from 100 to 2000 nm. These macropores create a macrochannel framework that facilitates the movement of gas molecules, enhancing mass transport and improving the accessibility of adsorption sites.[60] Various phophonate linkers as listed in Table 2 have been utilised to synthesize adsorbent materials, including Ti–HE, Ti–BH, Ti–HP, Ti–PA, Ti–DT and Ti–PB. The P–O–Ti bonding enhances the stability of the adsorbent material and its capacity to interact with ammonia through acid–base reactions. This hierarchical design, integrating large macropores for effective gas diffusion with mesopores for increased surface area, significantly enhances the material's ammonia adsorption efficiency. Transmission electron microscopy (TEM) images (A–D) confirm the presence of microchannels with walls composed of nanoparticles. The enhanced surface area is attributed to macropores interspersed with a wormhole-like mesophase (2 to 8 nm in size), which further optimizes the adsorption process. Notably, in Ti–HP, the macroporous network walls are composed of mesophase structures formed by aggregated nanoplates, which are approximately 25 nm in size.

Alshareef *et al.* reported the synthesis of one-dimensional titanium phosphonate nanowires (TiPNWs), where the unique morphology facilitates charge carrier transport, playing a pivotal role in photocatalysis.[63] These nanowires, approximately 80 nm in diameter, exhibit an amorphous nature with smooth surfaces. The homogeneous incorporation of etidronic acid (EA) into the Ti–O cluster influences the structural integrity, contributing to the material's robustness and electronic properties. Phosphonate groups derived from the organophosphonic acid form strong bonds with the titanium-oxo clusters, imparting superior stability, compared to MOFs utilising carboxylate linkers. Most intriguing aspect reported in this study is the bandgap engineering, attributed to electron-donating hydroxyl groups (–OH), which enable narrowing the bandgap more effectively than –Br in TiPNW–Br.

Hybrid porous titania phosphonate materials incorporating various functional groups (octyl, propyl, and phenyl) are synthesized using titania scaffolds that serve as the inorganic backbone of the hybrid network.[65] The titania framework is functionalized with diphosphonic acids modified with organic groups such as octyl (C8), propyl (C3) and phenyl (Ph), which are bonded strongly to TiO_2 *via* Ti–O–P linkages. These organic linkers are responsible for both the chemical stability and the surface functionalization of the material. For instance, a long alkyl chain introduces hydrophobicity and leads to the formation of layered structures with large pores whereas a shorter alkyl chain is responsible for flexible structures with controlled porosity. The layered morphology is further influenced by van der Waals interactions between extended organic chains, while the rigidity and potential π–π stacking interactions induced by aromatic groups impact molecular packing and porosity. The hybrid materials form nanosized particles with porous architectures, and it is observed that the porosity depends on both the type and concentration of the phosphonate precursor. 31P NMR analysis confirms multiple binding modes (mono-, bi-,

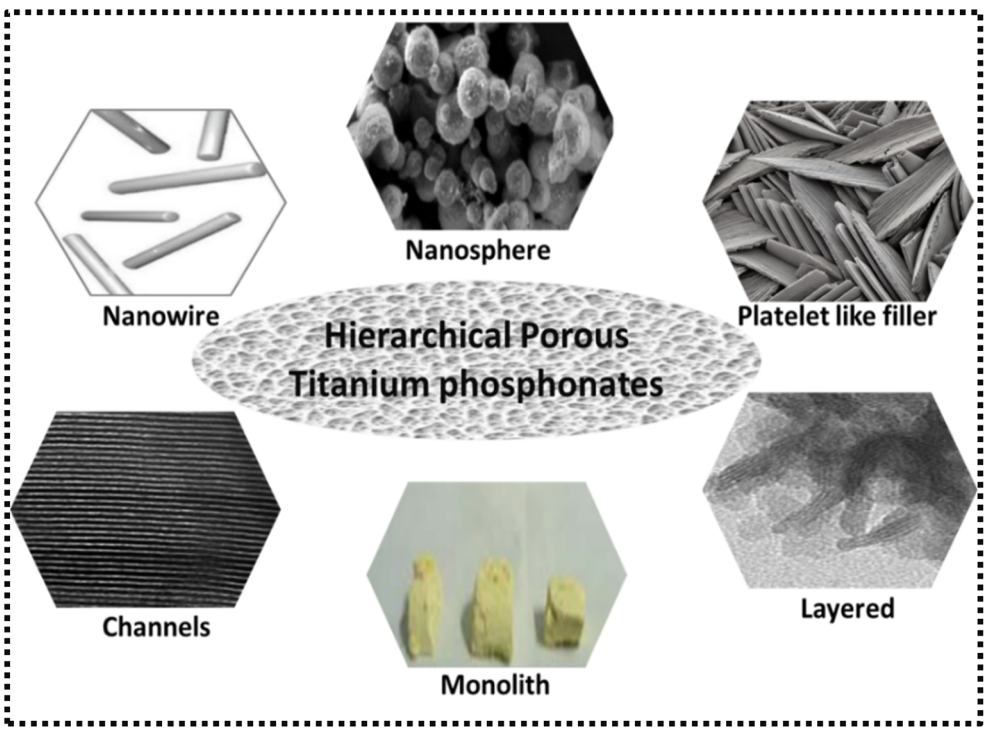

Fig. 6 Morphological variations in HPTPs.

and tridentate) for the phosphonate groups, significantly influencing the structural integrity and functional properties of the framework materials. These materials exhibit mesoporous architectures, with tunable pore sizes ranging from microporous to mesoporous depending on the functional groups and synthesis conditions employed. Furthermore, the study reveals that the crystallinity of the sample depends on higher ratios of Ti to phosphonate (Ti/2P). The incorporation of organic components increases the crystallinity, promoting the formation of a prominent anatase phase, with rutile and brookite phases also observed; this affects the porous nature, surface area, and catalytic efficiency. However, at lower Ti/2P ratios, the titania phase remains predominantly amorphous due to the extensive surface coverage by diphosphonic acids, which impedes crystalline phase formation. This effect is more pronounced with alkyl-based diphosphonic acid compared to phenyl phosphonic acid. The structural features underscore their morphological versatility (Fig. 6) and highlight their potential applications in separation technologies, catalysis, adsorption studies, *etc*.

4. Role of ligand selection in achieving well-defined structure and pore chemistry

The rational design of porous framework structures emphasizes the careful selection of metal nodes and organic precursors, as these components are fundamentally linked to the structural features and functionality of hybrid materials. The key challenge lies in identifying the optimal combination to achieve the desired intrinsic properties in functionalized target molecules, with precise control over position and orientation.[71] Another critical aspect of ligand selection is its influence on the coordination geometry within the first coordination sphere, which directly controls activity regulation, while the second coordination sphere facilitates non covalent bonding and structure stability. Phosphonate precursors (Table 2) acting as potential O-donors successfully generate organic/inorganic building blocks with diverse topologies, including MOFs, clusters, coordination polymers, *etc*. The nature of the phosphonate functional groups further modulates the material's properties: alkyl groups/chains increase the flexibility within the hybrid framework, whereas aromatic ring-substituted phosphonic acids impart rigidity due to their delocalised pi electrons, reinforcing structural stability.

Organophosphonic linkers (Table 2) play a crucial role in the band gap, due to the strong donating ability of –OH functionality. The incorporation of multifunctional groups within these linker such as di, tri or tetra phosphonic acids enhances the material's performance. Additionally, heterofunctional moieties are sometimes introduced to achieve hierarchical structural advantages. In ligands such as HPAA and PBTCA, the phosphonate and carboxylate groups may not coordinate simultaneously, leaving unsaturated coordination sites available as active centers for pollutant or heavy metal ion capture. Similarly, polydentate claw-type molecules, including EDTMPS, DTPMPA, BHMTPMPA, and PAPEMP, contain alkyl-bridged nitrogen donors, which enhance coordination and interaction, ultimately improving catalytic and adsorption efficiency in cost-effective multifunctional materials. The strong P–O–Ti bonding in various PTPs highlights the robust coordination ability of these linkers, often forming doubly or triply bridged binding modes observed in cage or cluster-type compounds. In HTiP-7, the BTPA ligand, featuring three $-P(O)(OH)_2$ groups, is designed to form $-P(O-Ti)_3$ units in the absence of Ti–O–Ti bonds, demonstrating the ligand's high affinity for titanium coordination. In polymer/titanium phosphonate (TP) nanocomposites, alkyl phosphonates such as DEOP act as fillers, while aryl phosphonates combined with a PS matrix generate layered fillers. In addition to this, in DEBP, the presence of $-CH_2$ enhances molecular mobility, reducing aggregation and leading to a well-defined structure. TiO_2–C8, utilizing alkyl-bridged diphosphonic acid (DPA), exhibits a flexible framework that enhances porosity and promotes the formation of layered structures—an effect not observed in propyl-bridged DPA. The reason may be the absence of van der Waals interaction in short propyl moieties associated with PrDPA, whereas PhDPA induces rigid, low-porosity structures.

Bulky polydentate ligands such as TPE and TPPhA, despite their inherent rigidity, contribute to intriguing porous architectures. Their organically pillared layered structures reduce close packing due to cross-linking effects, leading to the formation of macro-/mesoporous channel walls interspersed with micropores. This hierarchical arrangement, developed with diverse surface functionalities, further enhances the material's applicability in adsorption and catalysis.

5. Potential applications of PTPs

Due to their hierarchical porosity ranging from microporous to macroporous phases, porous titanium phosphonates (PTPs) have demonstrated remarkable potential for a variety of applications. Although receiving less attention compared to other hybrid materials, their applicability and performance relative to traditional hybrids possessing uniform porosity are astounding. This section reports the novel applications of hierarchical porous titanium phosphonates (HPTPs) in energy storage, catalysis, ion exchange, sensing, adsorption, and others relying on the structural hierarchy.

5.1 PTP/HPTPs as catalysts

Hierarchical titanium phosphonates are of considerable interest as catalysts due to their unique porosity, which facilitates efficient mass transfer and diffusion of reactants and products. Further optimization of the porous architecture enhances the functional efficiency by selectively tailoring the catalytic environment, increasing the number of active sites, and improving the accessibility of the catalytic centres for practical applications. Photocatalytic hydrogen evolution using hybrid porous materials, such as clusters or Metal–Organic Frameworks (MOFs) as catalysts, is a burgeoning arena in sustainable energy research, offering viable alternatives to

minimise resource consumption and promote green reactions.[72,73] Photocatalysts absorb light with energy equal to or greater than their bandgap energy, causing electron excitation with electron–hole pair formation followed by charge migration and inhibition of recombination to retain catalytic activity. In processes, such as the hydrogen evolution reaction (HER) from water, under light irradiation, the goal is to produce hydrogen, a clean and renewable energy source, by harnessing solar energy. The enhanced catalytic efficiency enabled by the hierarchical porosity of the HPTPs plays a crucial role in this reaction, as their well-defined porosity facilitates optimal light absorption, charge separation, and mass transport, ultimately improving hydrogen production efficiency.

Li *et al.* reported titanium phosphonate-based MOFs for enhancing the photocatalytic hydrogen evolution reaction (HER).[53] Hierarchically mesoporous titanium phosphonates (HM-TiPPh) and mesoporous titanium phosphonate materials (M-TiPPh) were synthesized for comparative studies, highlighting the critical role of the anionic polymer poly(acrylic acid) (PAA) in forming hierarchical porosity. They found that the materials favoured mass transfer and exhibited strong optical absorption during the photocatalytic water splitting for hydrogen production. Under visible light irradiation (λ > 400 nm, Fig. 7a), a remarkable H_2 production rate of 945 μmol h^{-1} g^{-1} is achieved on HM-TiPPh, surpassing that of TiO_2 (249 μmol h^{-1} g^{-1}). In contrast, M-TiPPh exhibits a lower mass-specific activity (698 μmol h^{-1} g^{-1}) than HM-TiPPh, underscoring the significant role of large secondary nanopores in enhancing the performance. The HM-TiPPh materials exhibited remarkable visible-light-driven hydrogen evolution activity and were even found to be superior to most of the TiO_2-based photocatalysts[74] and other catalytic systems.[75,76]

On subsequent exposure to full-spectrum simulator illumination (Fig. 7b), HM-TiPPh exhibits a remarkable hydrogen production rate of 1873 μmol h^{-1} g^{-1}, 1.58 and 3.21 times greater than that of MTiPPh (1185 μmol h^{-1} g^{-1}) and TiO_2 (584 μmol h^{-1} g^{-1}), respectively, aligning with the pattern observed under visible light irradiation. HM-TiPPh exhibited excellent long-term stability, maintaining its activity after four consecutive cycles under prolonged light exposure for 16 h. These findings highlight material's superior hydrogen evolution performance under both visible light and simulated full spectrum illumination, as shown in Fig. 7.

Macroporous titanium phosphonate (TOP) materials, with a pore size around 400 nm, exhibiting remarkable photocatalytic activity and heavy metal ion adsorption characteristics are reported.[56] Three-dimensionally ordered macroporous titanium phosphonate materials developed by an inverse opal method using the HEDP precursor, TOP and β-cyclodextrin (β-CD) added derivative (TOPβ), containing hydroxyethylidene groups inside the frameworks are the focus of the comparative study. The inorganic–organic hybrid materials exhibit significant photocatalytic activity, as demonstrated by the photodecomposition of Rhodamine B (RhB).

Fig. 8 illustrates that while TOP exhibits slightly lower efficiency than the commercial P-25, TOPβ demonstrates superior catalytic activity, despite having a higher band gap of TOPβ (3.19 eV) compared to P-25 (3.10 eV). This discrepancy is likely attributed to the pore-wall structure of the synthesized photocatalysts. The macroporous titanium phosphonate material is comparable in size to the wavelength of light, facilitating enhanced photon energy supply to the inner surface. The 3D-ordered macropores with internal windows serve as light-transfer pathways, enabling deeper light penetration into the photocatalyst.[75] Furthermore, doping phosphorus into the framework of the synthesized materials enhances photocatalytic efficiency.[77–79] Due to the extended band gap energy of phosphonate based materials, mesoporous TiO_2 exhibits higher photocatalytic activity than P-25.

Similarly, EDTMPS, a polydentate claw molecule, forms a hexagonal structure PMTP-1 with well-ordered periodic mesopores with an average pore size of 2.8 nm, and a surface area of

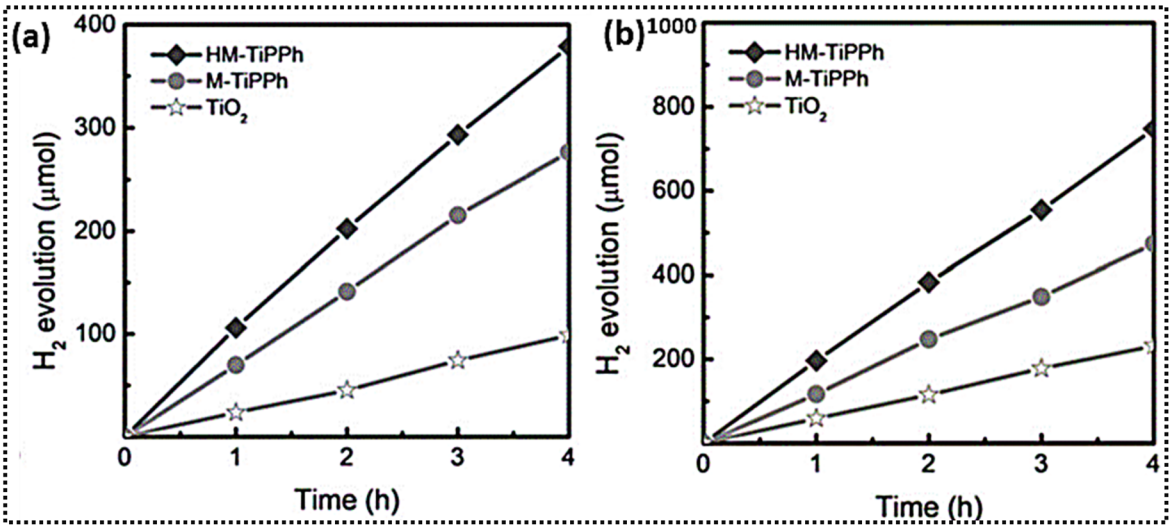

Fig. 7 (a) Typical time course of hydrogen evolution catalyzed by the synthesized photocatalysts under visible light irradiation and (b) under simulated sunlight. Adapted with permission from ref. 53. Copyright of Wiley, 2018.

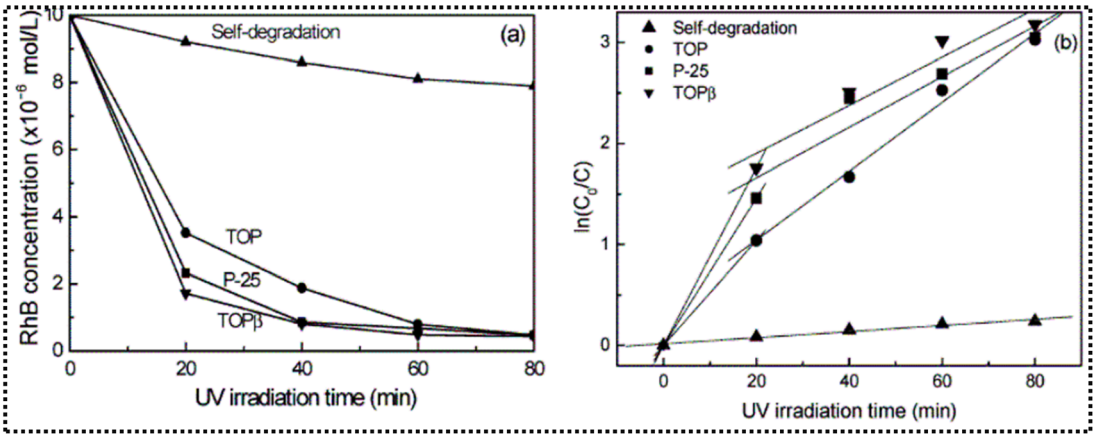

Fig. 8 (a) Photocatalytic activities of the samples for RhB degradation under UV-light irradiation; (b) Plots of $\ln(C_0/C)$ *vs.* the irradiation time, showing the fitting results using the pseudo-first-order reaction. Adapted with permission from ref. 56. Copyright of American Chemical Society, 2008.

1066 m^2 g^{-1}.[59] The material exhibits enhanced photocatalytic activity, particularly in the degradation of organic compounds such as RhB, outperforming commercial photocatalysts like P-25. A degradation rate of 68.4% results from high absorption phenomena and a well-structured mesophase with a high surface area, providing more active sites for photoabsorption and mass transfer. CuO nanoparticles, dispersed on hybrid or inorganic supports, exhibit high oxidation activity, as shown in Fig. 9. CuO-MTPs demonstrate stability in low-temperature oxidation reactions compared to other phosphonate hybrids, whereas CuO-iTP shows a 4% decrease in the conversion rate during the first 2 h, followed by stability; this may be due to the reaction between the reactant and the catalyst.

The robust 1D nanowire morphology of titanium phosphonate photocatalysts facilitates charge carrier separation and transport while reducing the band gap. This structural advantage enables the development of advanced, rationally functionalized catalysts with superior structural compatibility and enhanced catalytic efficiency. As shown in Fig. 10c functionalisation of the phosphonate precursor by replacing –OH with a weak electron donor, such as –Br, results in reduced photocatalytic hydrogen production in TiPNW–Br compared to TiPNW, highlighting the crucial role of the –OH functionality.[63] Moreover, the Ti–O–P bonding acts as a vital connection between phosphonic bridging groups and the titanium oxo core, contributing to the material's stability, outperforming TiO_2. The study demonstrates the possibility of bandgap tuning in TiPNW materials, where structural modification followed by ligand functionalisation plays a crucial role in optimizing electronic properties (Fig. 10b). The presence of an electron-donating group (-OH) in the linker raises the Valence Band Maximum (VBM), effectively lowering the band gap relative to TiO_2. In contrast, an electron electron-withdrawing group (–Br) lowers the VBM with an increase in the bandgap, which is confirmed by DFT calculations. The optimized VBM–CBM alignment in TiPNWs facilitates charge separation, reducing recombination losses. The lower bandgap enhances visible light absorption, ultimately increasing the photocatalytic conversion efficiency. TiPNWs exhibit superior photocatalytic activity compared to TiPNPs as evidenced by their higher hydrogen

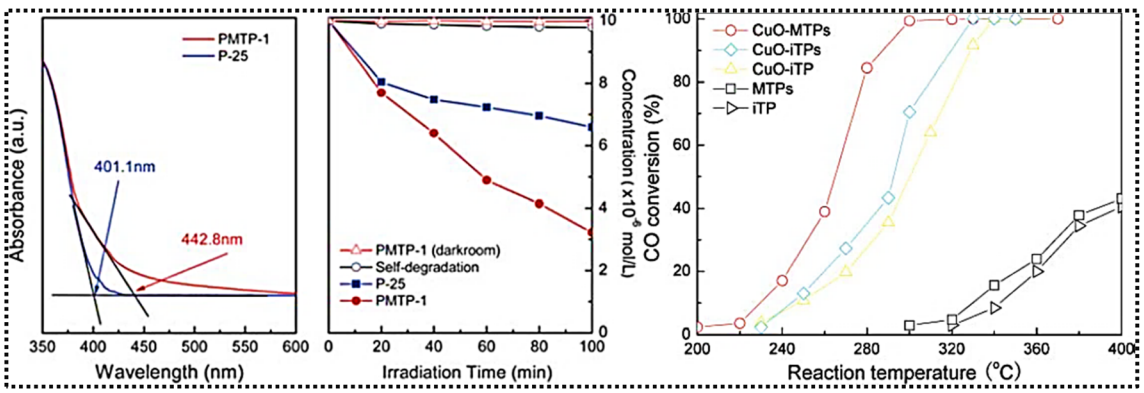

Fig. 9 UV-vis diffuse reflectance spectra of PMTP-1 and commercial P-25 (left), and photocatalytic activities of PMTP-1 and P-25 for RhB degradation under analogous solar light irradiation (2nd left). Catalytic activity for CO oxidation (right). Adapted with permission from ref. 59. Copyright of Royal Society of Chemistry, 2010.

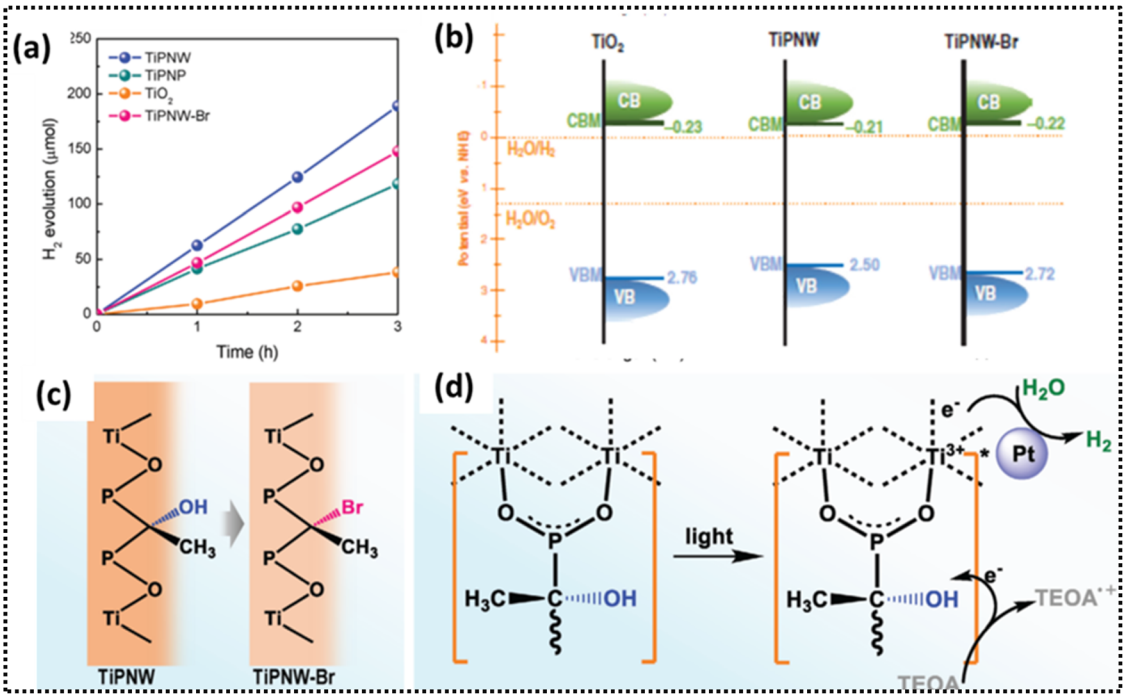

Fig. 10 (a) Typical time course of hydrogen evolution catalyzed by the synthesized photocatalysts in comparison with TiO_2 under visible light irradiation. (b) Pictorial representation of the electronic band structure of TiO_2, TiPNWs and TiPNW–Br. (c) Schematic view of the formation of TiPNW–Br. (d) Proposed mechanism for H_2 production. Adapted with permission from ref. 63. Copyright of Wiley, 2020.

production rate of 1260 μmol h^{-1} g^{-1}, significantly surpassing TiPNPs' 501 μmol h^{-1} g^{-1}.

Although both possess similar coordination environments and TiPNPs possess a higher surface area, the 1D nano wire morphology plays a pivotal role in the enhanced performance. A full spectrum simulator demonstrates a high hydrogen evolution rate which is 2346 μmol h^{-1} g^{-1} for TiPNWs and 955 μmol h^{-1} g^{-1} for TiPNPs. Hence this finding confirms that the surface area alone is not responsible for good catalytic activity as TiPNPs with a large surface area feature a lower hydrogen evolution rate in comparison to TiPNWs, underscoring the critical role of the nanostructure and morphology of the synthesized catalyst (Fig. 10a). Besides this the cocatalyst platinum (Pt) ensures efficient electron extraction at the conduction band of the Ti-oxo cluster by capturing and spatially separating the photoinduced electrons (Fig. 10d). This prevents rapid recombination with holes at organic ligands, thereby dramatically enhancing charge carrier dynamics and overall photocatalytic efficiency.

Furthermore, stability studies reveal that TiPNWs maintain their photocatalytic activity over five consecutive cycles of 3 h operation without degradation or deactivation. Additionally, the catalyst also retains its morphology after two months of storage, demonstrating robustness and long term stability of the material.

T. Ma and S. Z. Qiao explored the role of periodic mesoporous metal phosphonates (PMMPs), comprising titanium phosphonates, as highly effective acid–base bifunctional catalysts.[64] These materials stand out due to their well-organized mesoporous structures, high surface areas, enhanced mass transfer and adjustable acid–base properties, making them valuable for heterogeneous catalysis. Mesoporous titanium phosphonates, Ti-AST, act as bifunctional catalysts, possessing both Lewis acid (P–OH) and Brønsted base (-NH_2) sites within their framework, which activate aziridine and CO_2, respectively, catalysing the cycloaddition reaction, as shown in Fig. 11. This dual functionality enables Ti-AST to facilitate acid–base cooperative reactions by forming reactive carbamate species. The cycloaddition process follows a highly regioselective path (98 : 2) due to the stability of the intermediate, resulting in selective oxazolidinone formation. Ti-AST exhibits outstanding catalytic performance, achieving a high conversion rate (>99%) and an impressive yield of 98%, surpassing most heterogeneous catalysts. Additionally, this reaction is both environment friendly and sustainable as it does not require halogens, organic solvents, or cocatalysts. Furthermore, Ti-AST is easily separable and reusable without any loss of activity, making it an efficient and practical catalyst for repeated use.

Overall, hierarchical porous titanium phosphonates (HPTPs) are very promising as highly effective catalysts, mainly due to their well-defined hierarchical porosity, high surface area, and structural tunability. These features synergistically enhance reactant diffusion, light harvesting, and catalytic site accessibility, leading to excellent catalytic efficiency and long-term stability. These advantages make HPTPs highly promising for practical applications in photocatalysis and other sustainable catalytic processes, surpassingthe limitations of conventional photocatalysts.

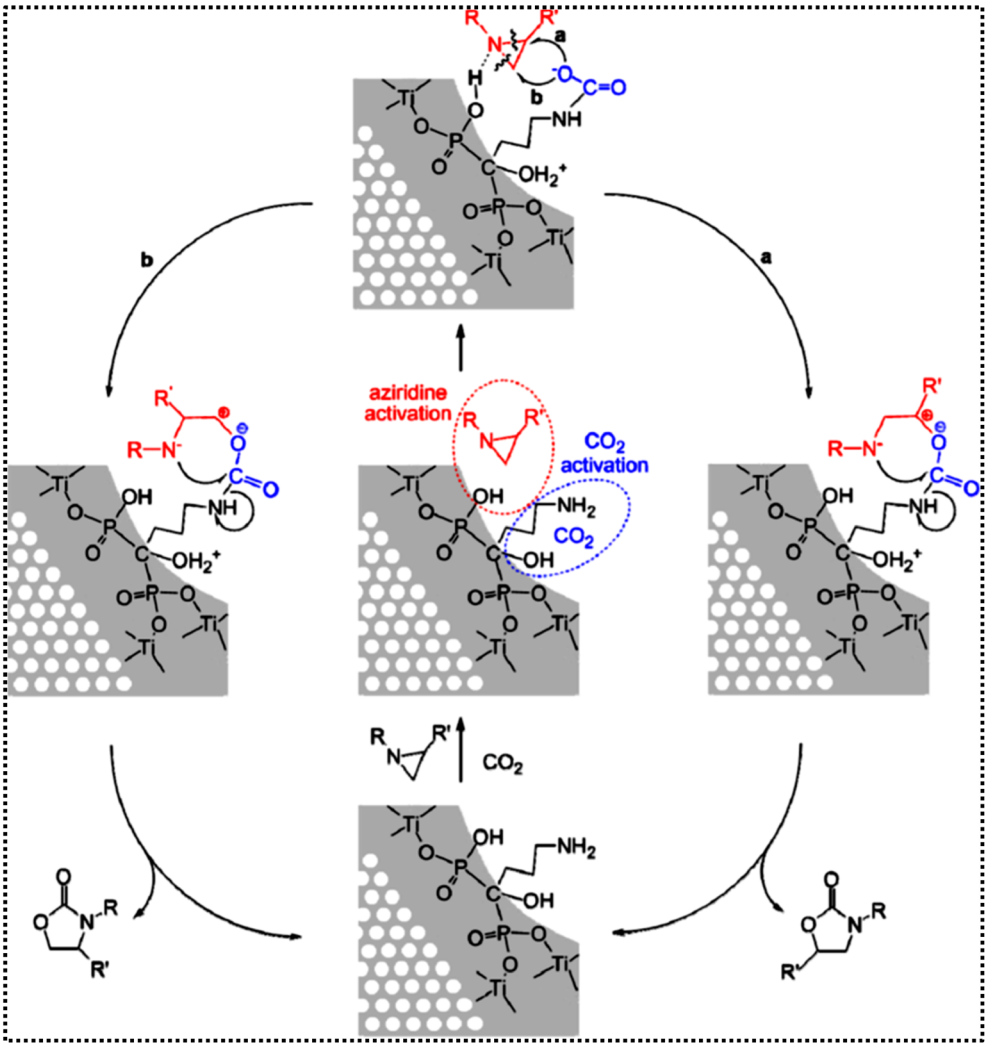

Fig. 11 Proposed reaction mechanism initiated on the bifunctional Ti-AST catalyst for the cycloaddition reaction between CO_2 and aziridine. Adapted with permission from ref. 64. Copyright of American Chemical Society, 2021.

5.2. Environmental remediation; pollutant adsorption/separation

Adsorption phenomena in porous solids play a crucial role in environmental remediation, particularly in applications such as CO_2 capture from industrial emissions, organic pollutant removal, heavy metal ion adsorption, *etc*. Phosphonate hybrid materials (PTPs) have emerged as effective adsorbents due to their unique structural attributes, combining organic and inorganic moieties to achieve high adsorption capacities, chemical stability, and selectivity for various pollutants, including heavy metal ions, *etc*. With increasing industrialization and urbanization, the release of heavy metal ions into the environment has become a major concern. When their concentrations exceed permissible limits set by the World Health Organization (WHO), they pose significant risks to ecological systems.[80,81] To address this, functional groups such as thiols, thiourea, and amines have been employed as metal ion binding motifs for the efficient removal of toxic heavy metals like Hg(II), Cu(II), and Cd(II). However, the potential of porous metal-organophosphate materials for heavy metal adsorption remains underexplored.[82,83] Porous structures are often considered as excellent adsorbents due to the availability of internal adsorption sites. In this process, the synthesis of crystalline nanoporous structures remains challenging as rapid aggregation often limits the development of permanent porosity, making it difficult to achieve stable and reusable materials.

PMTP-1, a periodic mesoporous titanium phosphonate, proved to be an efficient adsorbent exhibiting Langmuir-type behaviour, with selective affinity towards Cu^{2+} ions over Pb^{2+} and Cd^{2+}.[54] Previously, mesoporous hydroxyethylidene-bridged metal phosphonate materials were investigated for their adsorption properties, but they exhibited relatively low surface areas (<511 $m^2\ g^{-1}$).[61] In contrast, PMTP-1 offers significantly improved performance featuring a high surface area of 1066 $m^2\ g^{-1}$. A key factor contributing to this enhanced adsorption

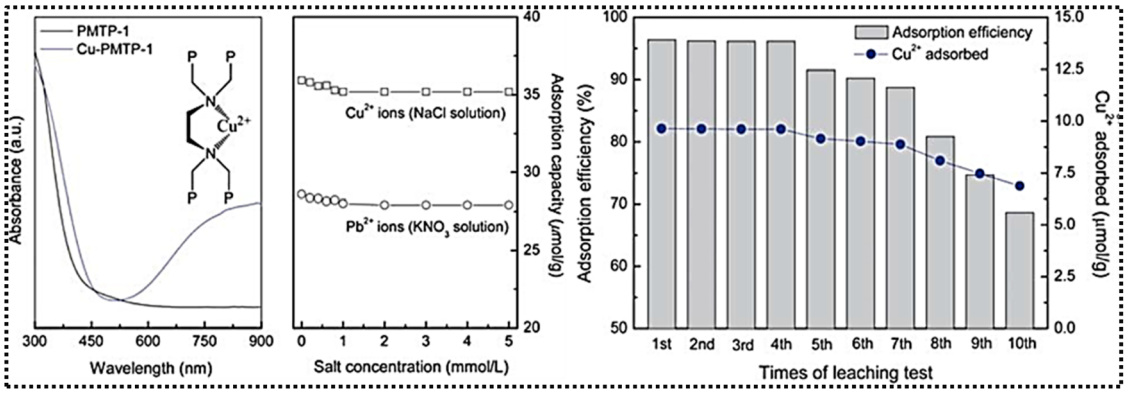

Fig. 12 UV-vis diffuse-reflectance spectra of the PMTP-1 adsorbent before and after Cu^{2+} ion loading (Cu-PMTP-1) (left). Effect of ion strength on metal ion adsorption behaviour (middle). Reusability of the PMTP-1 adsorbent for Cu^{2+} ions (0.2×10^{-4} mol L^{-1}) (right). Adapted with permission from ref. 59. Copyright of Royal Society of Chemistry, 2010.

capability is the presence of ethylene diamine bridging groups from EDTMPS, which exhibit a strong affinity for Cu^{2+} ions. Additionally, the high distribution coefficient parameter (Kd) for Cu^{2+} further supports the preferential adsorption of Cu(II), making PMTP-1 a highly effective and selective material for heavy metal ion removal.[84,85]

The material remains reusable upto four cycles (96.4% uptake efficiency) even under strong acidic conditions (1 M HCl) sustaining multiple sorption cycles as depicted in Fig. 12 (right). The presence of external electrolytes, such as NaCl for Cu^{2+} and KNO_3 for Pb^{2+} increases ionic strength, but results in only a minimal decrease in adsorption efficiency up to 1 mM strength;thereafter the adsorption efficiency shows static behaviour even at high electrolyte concentrations (Fig. 12, middle). Another mesoporous titanium phosphonate (MTP) integrated with the EDTMPS ligand possessing a surface area of 606 m^2 g^{-1} and containing macrovoids within microspheres, has been reported to exhibit monolayer adsorption of Cu^{2+} due to the strong ligand coordination.[62] The adsorption capacity was found to be 38.41 μmol g^{-1}, comparable to those of previously reported periodic mesoporous organosilicas.[86,87] Similarly, heavy metal ion adsorption by amorphous macroporous titanium organophosphonate materials (TOP and TOPβ adsorbents) in mixed solutions containing Cu(II), Cd(II), and Pb(II) ions at the same concentration (10 mg L^{-1}), demonstrated a distinct preference for the uptake of Cu^{2+}.[51] The adsorption capacity for Cu^{2+}(0.157 mmol g^{-1} for TOP and 0.166 mmol g^{-1} for TOPβ) was significantly higher than that for Cd^{2+} (0.064 mmol g^{-1} for TOP and 0.070 mmol g^{-1} for TOPβ) and Pb^{2+}(0.045 mmol g^{-1} for TOP and 0.046 mmol g^{-1} for TOPβ). The percentage removal of Cu^{2+} was approximately 20%, whereas the removal of Cd^{2+} and Pb^{2+} was around 10%. Porous MOF materials have been widely studied for absorption and separation techniques, as organic/inorganic functional groups facilitate strong interaction with contaminants or pollutants. Yaghi *et al.* conducted extensive research on the porosity of various MOF materials.[88–90] Later on, composite adsorbents with a combination of organic and inorganic phases demonstrated excellent adsorbent behaviour, particularly for ammonia gas adsorption (5.2 mol kg^{-1}), as reported by Levan *et al.*[91]

The hierarchical porosity of these materials enhances their adsorption efficiency, making them promising candidates for pollutant decontamination. Ammonia adsorbents based on phosphonate precursors (organophosphonic acids) and

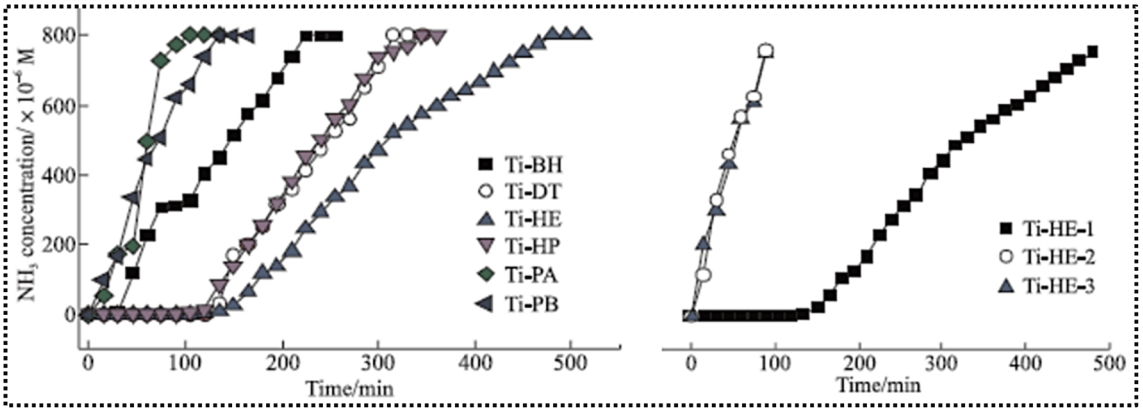

Fig. 13 NH_3 adsorption efficiency of PTPs (left) and three cycles of NH_3 adsorption measurements for Ti-HE. Adapted with permission from ref. 60. Copyright of Wuhan University of Technology and Springer Verlag Berlin Heidelberg, 2017.

hydrolysed metal alkoxides have led to the development of hierarchical PTPs, which have been subjected to adsorption studies.[60]

Among the six HPTPs, Ti–PA and Ti–PB have monolith structures with relatively small surface areas, whereas Ti-HP possesses the highest surface area (401 $m^2\ g^{-1}$) among all the Ti–X hybrids. Ti-HE, on the other hand, features the highest saturation adsorption capacity (75.2 mg g^{-1} (Fig. 13). The presence of hierarchical pores, surface adsorbed water, and hydroxyl groups enhances the saturation adsorption time and improves NH_3 adsorption performance. Although both physisorption (*via* van der Waals forces) and chemisorption (*via* acid–base reactions between ammonia and acidic sites) contribute to the adsorption process, the overall efficiency primarily depends on chemisorption. This mechanism restricts desorption, preventing secondary pollution and making these materials highly effective for environmental remediation. Consequently, these innovative materials are categorised as adsorption-reaction-type materials.

Another example of hierarchical macroporous morphology within a mesoporous framework is observed in TPPH-P123 and TPPH-F127, which exhibit high surface areas and exceptional sorption capacities for Cu^{2+} in the liquid phase and CO_2 in the gas phase, highlighting their potential for environmental remediation.[61] The hierarchical structure of these hybrid frameworks helps maintain the specific surface areas at the pore system level, ultimately enhancing sorption capacity. The high distribution coefficient (K_d) values (92 405 ml g^{-1} for TPPH-P123 and 232 273 ml g^{-1} for TPPH-F127) indicate a favorable environment for Cu^{2+} adsorption (Fig. 14a). Bridging phosphonates play a pivotal role with methylene –OH and P–O groups from HEDP providing coordination sites that enhance sorption ability. Additionally, macro channels combined with mesophases facilitate diffusion and mass transfer, further improving adsorption efficiency. Between the two hybrids, TPPH-P123 with its high surface area, proves to be a superior adsorbent. It also demonstrates excellent reusability, maintaining a 96.45% uptake efficiency even after four cycles (Fig. 14c). Interestingly pH studies reveal that the optimal absorption conditions occur in a neutral environment (pH = 7), with a sharp decrese in uptake capacity observed as the pH increases further (Fig. 14b).

Similarly, various adsorbents like activated carbon, mesoporous silica and zeolite-type materials have been widely studied for gas phase adsorption and separation techniques in the environment remediation processes. However, PTPs are also gaining significant attention for greenhouse gas adsorption, particularly CO_2, due to their advanced structure, functional properties, and superior adsorption performance. As depicted in Fig. 14d, thermogravimetric analysis (TGA) results for adsorption studies show that the initial adsorption rate is slow and thereafter it reaches equilibrium, likely due to the physisorption process. At 35 °C, TPPH-P123 exhibits a CO_2 uptake of 0.75 mmol g^{-1} whereas TPPH-F127 shows 0.63 mmol g^{-1}. Both values surpass the adsorption capacities of silica based adsorbents with high specific surface areas, highlighting the advantage of these hybrid materials. The presence of van der Waals forces between CO_2 molecules and the hybrid framework further enhances the adsorption process. Additionally, the incorporation of the organic functional groups and the

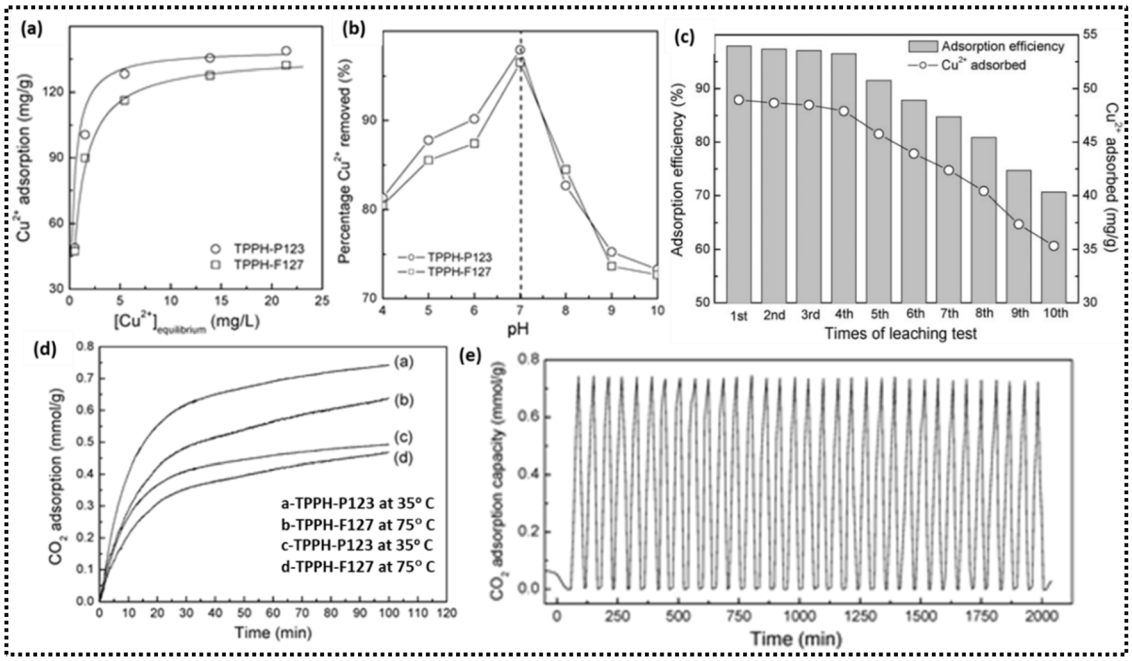

Fig. 14 (a) Cu^{2+} adsorption isotherm for TPPH hybrid materials. (b) Effect of pH on Cu^{2+} removal by the TPPH material. (c) Reusability of the adsorbent TPPH-P123 for Cu^{2+} ions (10 mg L^{-1}). (d) TGA records for CO_2 adsorption. (e) Multiple cycles of CO_2 adsorption measurements. Adapted with permission from ref. 61 Copyright of Royal Society of Chemistry, 2010.

morphological properties of the materials, play a major role in enhancing adsorption efficiency. The micro-morphology of macrochannels reduces resistance and facilitates mass transfer, making these porous materials more effective for achieving adsorption/desorption equilibrium. Furthermore, hierarchical TPPH hybrids demonstrate excellent reusability, as their adsorption/desorption capacity remains undisturbed up to 33 consecutive cycles, proving their robustness and long-term efficiency as practical adsorbents.

The sorption behavior of alkyl-functionalized hybrid titania phosphonates, incorporating octyl (C8), propyl (C3), and phenyl groups, has also been investigated based on three different diphosphonic acids.[65] Solid-phase extraction experiments were carried out using methanol/heptane for C3- and C8-functionalised systems, while a methyl/pyridine mixture was used for the phenyl functionalised system. Among these materials, TiO_2–C8 demonstrated excellent separation performance due to its layered structure, which prevents strong interaction with heptane molecules, thereby facilitating separation. In contrast, TiO_2-Ph-5 exhibited poor separation efficiency, retaining 100% of pyridine, which may be ascribed to the strong interaction between methanol and pyridine. Compared to commercially available silica C8-columns, alkyl functionalised titania hybrids show superior efficiency in purifying waste streams and contaminated water sources, making them promising materials for environmental remediation.

5.3. Miscellaneous applications

5.3.1 Sensing. Porous materials with multifaceted applications address critical challenges in the energy and environment sectors. Their tunable frameworks exhibit nonlinear optical properties, such as enhanced conductivity and pollutant sensing, while ensuring improved water stability. In this context, the combination of high-oxidation state metals and aromatic linkers plays a crucial role in sensing mechanisms. Detecting explosives like 2,4,6-trinitrophenol (TNP) is particularly challenging, especially at trace levels, due to its strong binding interactions and low fluorescence response. Being highly soluble in water, TNP poses a significant environmental and health risk, as it can easily penetrate living systems. Fluorescent sensors are among the most widely used detection methods, offering an eco-friendly, cost-effective, and highly sensitive approach for identifying TNP even at trace levels. Porous MOF materials, with their high specific area, exceptional selectivity, chemical versatility, and luminescent properties, effectively enhance sensing capabilities. In addition, porous nanomaterials such as MOFs, COFs, COPs, and POPs have garnered significant attention due to their potential applications in sensing organic pollutants and metal ions. Apart from this, these targeted materials are primarily designed for recyclability and high specific capacitance, making them highly efficient for sustainable applications. Although organic and inorganic phosphates have been widely reported as sensors, phosphonate MOFs remain relatively unexplored in this field.[92]

Chakraborty *et al.* reported a novel tetradentate phosphonate ligand-based porous metal–organic framework, H_8L-Ti-MOF, which was for the selective sensing of 2,4,6-trinitrophenol (TNP) in the aqueous phase.[9] The fluorescence intensity of the MOF was completely quenched upon coming in contact with TNP, while other nitroaromatic and nitroaliphatic compounds had only a minimal impact on its fluorescence profile. Although the quenching mechanism is attributed to one of the three possible pathways – Photoinduced Electron Transfer (PET), Resonance Energy Transfer (RET) and Intermolecular Charge Transfer (ICT) – the electron-rich polyaromatic system interacts with TNP *via* –C–H$\cdots\pi$ and $\pi\cdots\pi$ interactions (Fig. 5). The observed bathochromic shift in fluorescence titration spectra supports the ICT mechanism, indicating charge transfer upon interaction. Due to the close proximity of the analyte, RET can't be ruled out as a possible mechanism to describe the host–guest interaction. Moreover, a dynamic quenching mechanism is suggested for the interaction, as confirmed by fluorescence lifetime experiments. Reusability studies indicate that the material remains effective for up to four cycles, with a detection limit of 3.6 μM (0.82 ppm).

5.3.2 Photoconductivity. PTPs, owing to their optoelectronic properties, respond to light and generate current, making them ideal for photoconductive applications. The micro/mesophase structure enhances electron and hole conductivity as they interact with the light source, undergoing excitation and subsequent recombination during the relaxation phase. In this photon-to-electron energy transfer process, the embedded porosity allows organic moieties (photosensitizers) to be trapped within the framework, further improving conductivity, which is not observed in TiO_2. Thus, the significant role of photosensitisers in PTPs and their intriguing structures was studied for the 1st time by Bhaumik and co-workers with the help of Rose Bengal (RB) dye encapsulated in tiny nanocrystals of self-aggregated HTiP-7 PTP.[55] The presence of mesovoids and microspheres contributes to exceptional carrier mobility and a high surface area of 255 $m^2\ g^{-1}$. As depicted in Fig. 15 (left), the RB-embedded PTP (HTiP-7RB) exhibits superior conductivity compared to HTiP-7 and benzene-1,3,5-triphosphonic acid (BTP). Light-driven photoconductivity studies, conducted by analysing the growth and decay of current at 10 V bias, reveal a current of 3.48×10^{-4} A for HTiP-7RB, significantly higher than 5.09×10^{-5} A for hybrid titanium phosphonate and 1.39×10^{-6} A for bulk titanium phosphate, highlighting the enhanced performance of the RB-embedded material. Thus, the incorporation of sensitizer molecules into porous semiconductor materials significantly enhances visible light-driven photoconductivity. Upon irradiation of HTiP-7RB with light, the optical excitation of RB facilitates electron injection from its excited state into the conduction band of the porous hybrid titanium phosphonate,[93] leading to improved charge carrier dynamics and overall performance.

This interfacial electron transfer takes place when optically excited RB injects electrons into the conduction band at a rate significantly faster than the decay of its excited (Fig. 15 right). In contrast, this phenomenon is absent in the hybrid titanium phosphonate and bulk titanium phosphate due to their large band gaps, where charge transfer occurs *via* the valence band. Thus, the incorporation of a photosensitizer molecule enhances

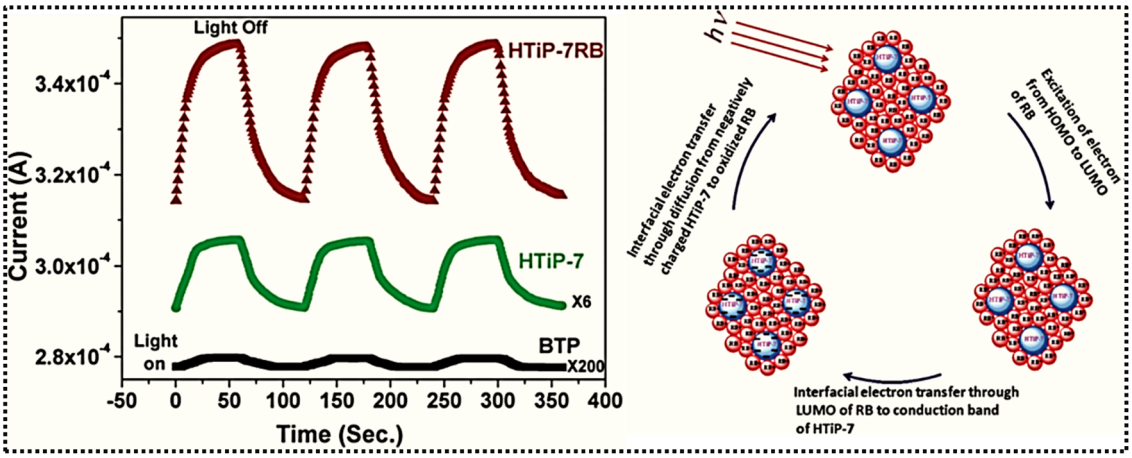

Fig. 15 Growth and decay current of BTP, HTiP-7, and HTiP-7RB (left). Schematic representation of electron flow in the dye-loaded HTiP-7 in the presence of light (right). Adapted with permission from ref. 55. Copyright of Royal Society of Chemistry, 2013.

electron excitation and transfer within the micro/meso pores of PTPs, thereby significantly boosting visible light-driven photocurrent generation.

5.3.3 Ion exchange. Ion exchange is another fascinating application of PTPs, playing a crucial role in environmental remediation, chemical separations, catalysis and energy storage. Their tunable porosity, high surface area, and diverse chemical functionalities make them highly efficient for selective ion exchange processes, enhancing performance in various applications. Organic–inorganic hybrids, composed of metal nodes bridged by organic linkers, offer a distinct advantage in ion exchange processes. Their well-defined pore and channel structures facilitate the selective trapping and exchange of cations or anions, making them highly effective for applications in separation, catalysis, and environmental remediation.[94,95]

Hybrid networks can be precisely tailored by functionalizing organic moieties to achieve the desired shape and size. This customization enhances the stability of functional materials, enabling their effective use even under extreme environmental conditions. In addition, the hierarchical porosity enhances the material's suitability by increasing its surface area. A prime example is the mesoporous titanium phosphonate monolith, PMTP-2, synthesized using 1-hydroxy ethylidene-1,1-diphosphonic acid (HEDP) as an anchoring molecule through an autoclaving process. This self-assembled structure exhibits a remarkably high surface area of 1034 m^2 g^{-1},[58] making it highly effective for various applications. Furthermore, the synthesized PMTP-2 was functionalized by sulfation with $ClSO_3H$, resulting in a significantly enhanced ion exchange capacity. This modification enables PMTP-2 to function not only as an efficient ion exchanger but also as a strong acid catalyst for certain low-temperature reactions. The facile sulfation process with $ClSO_3H$ leads to the formation of stable hydrosulfated esters, which is likely attributed to the specific alkyl hydroxyl structure of the coupling molecule HEDP. During the subsequent synthesis of the ordered mesophase, carbon-hydroxyl groups were uniformly distributed across the pore walls. These hydroxyl groups were then functionalized with SO_3H groups through treatment with $ClSO_3H$, enhancing the material's ion exchange and catalytic properties (Fig. 16).

This functionalization significantly enhances the ion exchange capacity compared to the unfunctionalized PMTP-2 and previously reported titanium phosphate materials, making it more effective for catalytic and separation applications.[56,96] For instance, sulfated PMTP-2s was employed for the esterification of oleic acid with methanol at ambient temperature and pressure, where PMTP-2s demonstrated superior activity compared to PMTP-2, achieving a conversion rate of

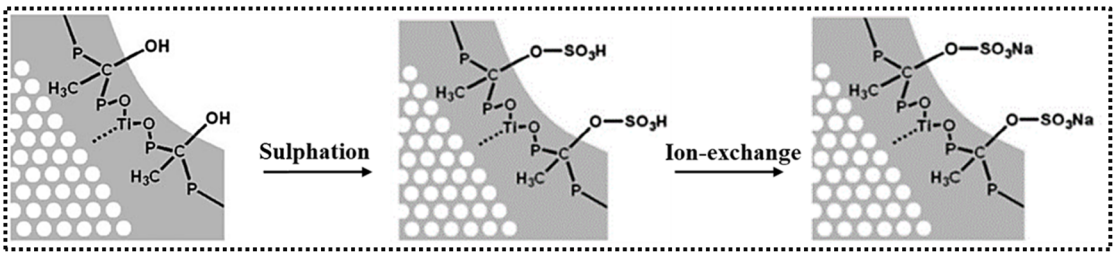

Fig. 16 Synthesis, sulfation and ion exchange processes of the monolithic PMTP-2 material. Adapted with permission from ref. 58. Copyright of Royal Society of Chemistry, 2010.

87.3%, significantly higher than that of unfunctionalized PMTP-2, which was only 4.9%. Furthermore, the conversion surpassed that of conventional sulfonic acid-functionalized mesoporous titania materials (81.7%).

5.3.4 Energy storage devices. Due to their tunable structure, high surface area, porosity, low charge transfer resistance, and shortened diffusion path for electrons or ions, PTPs are highly suitable for energy storage devices. Their structural integrity and stability enhance the device's charge/discharge cycles, improving electrolytic performance and enabling their use as supercapacitors.[97–99] Porous MOF materials with a high specific surface area coated on conductors enhance electrochemical performance. They can also serve as cathodes or anodes, where the redox-active metal centers contribute to lithium-ion storage.[100,101] Hydrogen storage is another crucial application, which is facilitated by various phosphonate-incorporated porous materials.[46] However, a major limitation of titanium(IV) phosphonates is their intrinsically low electrical conductivity, which considerably influences their efficiency in energy storage devices. Unlike conductive MOFs or MOF-derived carbon materials, titanium(IV) phosphonates necessitate composite formation with conductive additives (*e.g.*, carbon black and graphene) for the improvement of electron transport. Additionally, metal doping can also be introduced within the framework to enhance conductivity. These structural modifications not only enhance porosity but also promote better ion diffusion and charge storage.

Furthermore, the hydrosulfated groups in PMTP-2s act as proton carriers, enabling their potential use as an electrolyte for fuel cells.[102] Similarly, H_8L-Ti-MOF, used as an electrode in an asymmetric supercapacitor, delivers 20.03 F cm^{-2} @0.1 mA cm^{-2} current density with excellent recyclability.[9] This energy storage capacity of the Ti-MOF was studied using an active material slurry coated on the cathode and a carbon black anode. While initial capacitance fading occurred up to 1000 cycles, only a 10% loss was observed over the next 900 cycles. The supercapacitive behaviour and 82.68% capacitance retention after 1000 cycles confirm the material's suitability for energy storage devices. As current density increases, galvanostatic charge/discharge (GCD) exhibits a slight deviation from ideal behaviour, indicating pseudocapacitance. The effect enhances the areal capacitance by enabling rapid, reversible redox processes combined with the usual electrostatic charge accumulation, increasing the energy storage ability.

5.3.5 Comparative stability analysis of titanium phosphonates and alternative materials. A comparative analysis of the stability characteristics of porous titanium phosphonates (PTPs) is presented, highlighting their performance in comparison with widely used porous materials, including activated carbons, zeolites, metal–organic frameworks (MOFs), and silica-based materials (*e.g.*, MCM-41 and SBA-15). These competing materials demonstrate thermal, chemical, mechanical, and hydrothermal stability, making them suitable for various applications as listed in Table 3. PTPs exhibit exceptional thermal stability (>500 °C) and outstanding chemical resistance under both acidic and alkaline conditions, making them highly suitable for use in catalysis, ion exchange, and

Table 3 Comparative analysis on the stability of PTPs and Other porous materials

Materials	Thermal stability	Chemical stability	Mechanical stability	Hydrothermal stability	Key applications	Ref.
PTPs	Highly stable (>500 °C)	Excellent (Resistant to acids and bases)	High (rigid framework)	High (stable in hot water/steam)	Catalysis, ion exchange, adsorption, and drug delivery	51 and 65
Activated carbons	Moderate (~800 °C under inert conditions)	Poor (oxidizes in strong acids/bases)	High (good mechanical strength)	Poor (degrades in humid environments)	Gas adsorption, water purification, and catalysis	103
Zeolites	High (>1000 °C)	Good (Resistant to acids but dissolves in strong bases)	High (robust crystalline structure)	Moderate (some structural degradation in hot water/steam)	Catalysis, ion exchange and molecular sieving	105 and 106
Metal–organic frameworks (MOFs)	Low to moderate (decomposes ~200–400 °C)	Poor to moderate (sensitive to moisture, acids, and bases)	Low to moderate (soft structure, fragile)	Poor (degrades in water/humid environments)	Gas storage, separation, catalysis and drug delivery	107 and 108
Silica-based materials (*e.g.*, MCM-41, SBA-15)	High (>800 °C)	Moderate (stable in weak acids but dissolves in strong bases)	High (porous but mechanically robust)	Moderate (some collapse in hot water)	Adsorption, catalysis and separation processes	109

adsorption.[51,65] In contrast, while activated carbons are remarkably mechanically robust, they can undergo oxidation under strongly acidic or basic conditions and tend to degrade in humid environments.[103] Zeolites offer excellent thermal and mechanical stability; however, their susceptibility to strong bases limits their applicability under highly alkaline conditions.[19] Although MOFs and COFs possess tunable porosity and structural versatility, they generally display poor hydrothermal stability and are prone to decomposition and structural collapse under aqueous or humid conditions. Similarly, silica-based materials such as MCM-41 and SBA-15 provide high porosity and moderate stability but are prone to dissolution in strongly alkaline solutions.[104]

Overall, PTPs emerge as a superior alternative due to their exceptional stability under diverse environmental conditions, making them particularly advantageous for applications that require highly durable and chemically resilient materials. This comparative study highlights TPs as a highly preferred, well-suited option for demanding environments where chemical and hydrothermal stability are essential.

6. Summary, conclusion, and future perspectives

Hierarchical porous titanium phosphonates (HPTPs) are regarded as a promising class of hybrid materials due to their unique combination of hierarchical porosity and tunable chemical properties, making them ideal for a wide range of applications in photocatalysis, environmental remediation and energy storage. This review particularly emphasizes the advantages of phosphorus-based linkers in addressing the hydrolytic stability issues often faced by traditional carboxylate-based materials. This review discusses various synthesis strategies—such as sol–gel, hydrothermal, and template-assisted methods—used to produce crystalline, amorphous, and paracrystalline HPTPs. It also outlines their structural characteristics, such as pore size distribution, crystallinity and surface area, and how these factors influence their performance in specific applications.

Furthermore, the review highlights recent advancements in the functionalization and modification of HPTPs to enhance their utility in industrial applications and environmental remediation processes such as pollutant adsorption and separation. Their high surface area, ordered mesostructures, and secondary pores enhance electrolyte and product transport, ensuring efficient light harvesting and exceptional photocatalytic performances. The pore architecture and the textural features can be finely tuned through various synthetic processes, ligand functionalisation and the incorporation of mixed ligands, such as N-donors and O-donors. Structure-directing agents significantly influence material porosity, enhancing pore size or inducing hierarchical structures for advanced photocatalytic systems. Multifunctional linkers with multiple binding modes further improve catalytic properties by directly affecting the coordination environment of the Ti(IV) centre.

High adsorption capacity and excellent reusability of HPTPs distinguish them as exceptional adsorbents for the environmental remediation process. Additionally, multiphase adsorption is observed, particularly in the liquid phase, where heavy metal ions and organic pollutants bind to functional groups within these hybrid materials. However, in gas phase adsorption, such as CO_2 or other gaseous pollutants, pore size and physisorption play a crucial role, relying primarily on non-covalent interactions like van der Waal's forces between the adsorbate and hybrid adsorbent molecules. In some instances, a combined effect of physisorption and chemisorption is observed. Additionally, metal ion adsorption studies underscore the significant influence of pH on the adsorption efficiency of PTPs and HPTPs.

Future research should aim to develop novel and sustainable synthesis strategies to improve control over hierarchical structures, understanding the interaction mechanisms between HPTPs and different reactants. Sensing, ion-exchange, photoconductivity, and electrochemical potential in energy storage devices are among the highlighted applications, although they remain relatively unexplored for PTPs/HPTPs. The primary challenge lies in addressing issues while achieving permanent porosity in hybrid materials. However, several key challenges remain, such as precise structural control, scalable production, and ensuring long-term stability under extreme conditions. PTPs also face limitations, including lower surface areas compared to zeolites and MOFs, which may limit their adsorption capacity, and the need for further assessment of mechanical strength under high pressure. Despite these challenges, PTPs excel in applications that require stability, particularly in acid-catalyzed reactions, pollutant adsorption and sensing.

Subsequent efforts should focus on integrating computational modelling and machine learning to design materials that predict and enhance porosity and stability in functional hybrid materials. The formulation of green synthesis approaches utilizing bio-derived precursors and solventless strategies would further promote sustainability. Also, incorporating other nanomaterials into HPTPs heterostructures could increase the usefulness of these materials in energy storage, photocatalysis, and environmental remediation. By addressing these challenges, HPTPs can evolve into materials of choice for next-generation functional devices with large-scale industrial implementation. Their robustness and tunability make them highly remarkable for industrial, environmental, and biomedical applications. Finally, emerging trends, key applications, and future directions in HPTP research are outlined, addressing current challenges and expanding their potentialin advanced materials science.

Data availability

Data will be made available on request.

Conflicts of interest

There are no conflicts to declare.

References

1 G. Cai, P. Yan, L. Zhang, H.-C. Zhou and H.-L. Jiang, Metal–organic framework-based hierarchically porous materials: synthesis and applications, *Chem. Rev.*, 2021, **121**, 12278–12326.
2 S. Kitagawa, Future porous materials, *Acc. Chem. Res.*, 2017, **50**, 514–516.
3 A. Ejsmont, J. Andreo, A. Lanza, A. Galarda, L. Macreadie, S. Wuttke, S. Canossa, E. Ploetz and J. Goscianska, Applications of reticular diversity in metal–organic frameworks: An ever-evolving state of the art, *Coord. Chem. Rev.*, 2021, **430**, 213655.
4 N. Hüsing, *Porous Hybrid Materials*, Wiley, Weinheim, 2006.
5 G. Férey, Hybrid porous solids: past, present, future, *Chem. Soc. Rev.*, 2008, **37**, 191–214.
6 R. Murugavel, A. Choudhury, M. G. Walawalkar, R. Pothiraja and C. N. R. Rao, Metal complexes of organophosphate esters and open-framework metal phosphates: synthesis, structure, transformations, and applications, *Chem. Rev.*, 2008, **108**, 3549–3655.
7 P. Bhanja and A. Bhaumik, Organic–inorganic hybrid metal phosphonates as recyclable heterogeneous catalysts, *ChemCatChem*, 2016, **8**, 1607–1616.
8 J. Panda, S. P. Tripathy, S. Dash, A. Ray, P. Behera, S. Subudhi and K. Parida, Inner transition metal-modulated metal organic frameworks (IT-MOFs) and their derived nanomaterials: a strategic approach towards stupendous photocatalysis, *Nanoscale*, 2023, **15**, 7640–7675.
9 D. Chakraborty, S. Bej, S. Sahoo, S. Chongdar, A. Ghosh, P. Banerjee and A. Bhaumik, Novel nanoporous Ti-phosphonate metal–organic framework for selective sensing of 2, 4, 6-trinitrophenol and a promising electrode in an energy storage device, *ACS Sustainable Chem. Eng.*, 2021, **9**, 14224–14237.
10 H.-B. Tai, S.-N. Lu, X. Zhang, Q.-W. Liu, Y.-N. Zhou, C.-Q. Jiao, Y.-Y. Zhu, C.-Y. Huang and Z.-G. Sun, Differently luminescent sensing abilities for Cu2+ ion of two metal phosphonates with or without the free Lewis basic pyridyl sites, *J. Mol. Struct.*, 2021, **1234**, 130175.
11 M. A. Nistor, S. G. Muntean, B. Maranescu and A. Visa, Phosphonate metal–organic frameworks used as dye removal materials from wastewaters, *Appl. Organomet. Chem.*, 2020, **34**, e5939.
12 S. S. Iremonger, J. Liang, R. Vaidhyanathan, I. Martens, G. K. Shimizu, T. Daff, D, M. Z. Aghaji, S. Yeganegi and T. K. Woo, Phosphonate monoesters as carboxylate-like linkers for metal organic frameworks, *J. Am. Chem. Soc.*, 2011, **133**, 20048–20051.
13 Y. Wei, K. A. Salih, M. F. Hamza, E. R. Castellón and E. Guibal, Novel phosphonate-functionalized composite sorbent for the recovery of lanthanum (III) and terbium (III) from synthetic solutions and ore leachate, *Chem. Eng. J.*, 2021, **424**, 130500.
14 Y. Zorlu, L. Wagner, P. Tholen, M. M. Ayhan, C. Bayraktar, G. Hanna, A. O. Yazaydin, Ö. Yavuzçetin and G. Yücesan, Electrically Conductive Photoluminescent Porphyrin Phosphonate Metal–Organic Frameworks, *Adv. Opt. Mater.*, 2022, **10**, 2200213.
15 P. Tholen, Y. Zorlu, J. Beckmann and G. Yücesan, Probing Isoreticular Expansions in phosphonate MOFs and their applications, *Eur. J. Inorg. Chem.*, 2020, **2020**, 1542–1554.
16 S. a. Ondrusova, M. Kloda, J. Rohlícek, M. Taddei, J. K. Zareba and J. Demel, Exploring the Isoreticular Continuum between Phosphonate-and Phosphinate-Based Metal–Organic Frameworks, *Inorg. Chem.*, 2022, **61**, 18990–18997.
17 R. Freund, O. Zaremba, G. Arnauts, R. Ameloot, G. Skorupskii, M. Dinca, A. Bavykina, J. Gascon, A. Ejsmont and J. Goscianska, The current status of MOF and COF applications, *Angew. Chem., Int. Ed.*, 2021, **60**, 23975–24001.
18 G. K. Shimizu, R. Vaidhyanathan and J. M. Taylor, Phosphonate and sulfonate metal organic frameworks, *Chem. Soc. Rev.*, 2009, **38**, 1430–1449.
19 L.-H. Chen, M.-H. Sun, Z. Wang, W. Yang, Z. Xie and B.-L. Su, Hierarchically structured zeolites: from design to application, *Chem. Rev.*, 2020, **120**, 11194–11294.
20 W. Li, J. Liu and D. Zhao, Mesoporous materials for energy conversion and storage devices, *Nat. Rev. Mater.*, 2016, **1**, 1–17.
21 L.-B. Sun, X.-Q. Liu and H.-C. Zhou, Design and fabrication of mesoporous heterogeneous basic catalysts, *Chem. Soc. Rev.*, 2015, **44**, 5092–5147.
22 D. W. Breck, *Zeolite Molecular Sieves: Structure, Chemistry, and Use*, 1974.
23 D. M. Chapman and A. L. Roe, Synthesis, characterization and crystal chemistry of microporous titanium-silicate materials, *Zeolites*, 1990, **10**, 730–737.
24 M. Taramasso, G. Perego and B. Notari, Preparation of porous crystalline synthetic material comprised of silicon and titanium oxides, *US Pat.*, US4410501A, 1983.
25 G. Alberti, P. Cardini-Galli, U. Costantino and E. Torracca, Crystalline insoluble salts of polybasic metals—I Ion-exchange properties of crystalline titanium phosphate, *J. Inorg. Nucl. Chem.*, 1967, **29**, 571–578.
26 S. Allulli, C. Ferragina, A. La Ginestra, M. Massucci and N. Tomassini, Preparation and ion-exchange properties of a new phase of the crystalline titanium phosphate, Ti (HPO4) 2· 2H2O, *J. Inorg. Nucl. Chem.*, 1977, **39**, 1043–1048.
27 A. I. Bortun, S. A. Khainakov, L. N. Bortun, D. M. Poojary, J. Rodriguez, J. R. Garcia and A. Clearfield, Synthesis and Characterization of Two Novel Fibrous Titanium Phosphates Ti2O (PO4) 2⊙ 2H2O, *Chem. Mater.*, 1997, **9**, 1805–1811.
28 C. Serre and G. Férey, Hydrothermal synthesis and ab initio structurfal approach of two new layered oxyfluorinated titanium (IV) phosphates: Ti 2 (PO 4) 2 F 4· N 2 C 2 H 10 (MIL-6) and Ti 2 (PO 4) 2 F 4· N 2 C 3 H 12· H 2 O, *J. Mater. Chem.*, 1999, **9**, 579–584.
29 A. Clearfield and J. Stynes, The preparation of crystalline zirconium phosphate and some observations on its ion

exchange behaviour, *J. Inorg. Nucl. Chem.*, 1964, **26**, 117–129.
30 C. M. Parlett, K. Wilson and A. F. Lee, Hierarchical porous materials: catalytic applications, *Chem. Soc. Rev.*, 2013, **42**, 3876–3893.
31 R. L. Siegelman, E. J. Kim and J. R. Long, Porous materials for carbon dioxide separations, *Nat. Mater.*, 2021, **20**, 1060–1072.
32 S. Chuhadiya, D. Suthar, S. Patel and M. Dhaka, Metal organic frameworks as hybrid porous materials for energy storage and conversion devices: A review, *Coord. Chem. Rev.*, 2021, **446**, 214115.
33 H. Li, T.-Y. Ma, D.-M. Kong and Z.-Y. Yuan, Mesoporous phosphonate–TiO 2 nanoparticles for simultaneous bioresponsive sensing and controlled drug release, *Analyst*, 2013, **138**, 1084–1090.
34 C. Serre, J. A. Groves, P. Lightfoot, A. M. Slawin, P. A. Wright, N. Stock, T. Bein, M. Haouas, F. Taulelle and G. Férey, Synthesis, structure and properties of related microporous N, N '-piperazinebismethylenephosphonates of aluminum and titanium, *Chem. Mater.*, 2006, **18**, 1451–1457.
35 C. Serre and G. Férey, Hybrid Open Frameworks. 8. Hydrothermal Synthesis, Crystal Structure, and Thermal Behavior of the First Three-Dimensional Titanium (IV) Diphosphonate with an Open Structure: Ti3O2 (H2O) 2 (O3P−(CH2)− PO3) 2⊙(H2O) 2, or MIL-22, *Inorg. Chem.*, 1999, **38**, 5370–5373.
36 C. Serre and G. Férey, Hydrothermal Synthesis and Structure Determination from Powder Data of New Three-Dimensional Titanium (IV) Diphosphonates Ti (O3P−(CH2) n− PO3) or MIL-25 n (n= 2, 3), *Inorg. Chem.*, 2001, **40**, 5350–5353.
37 H. Assi, G. Mouchaham, N. Steunou, T. Devic and C. Serre, Titanium coordination compounds: from discrete metal complexes to metal–organic frameworks, *Chem. Soc. Rev.*, 2017, **46**, 3431–3452.
38 J. Goura and V. Chandrasekhar, Molecular metal phosphonates, *Chem. Rev.*, 2015, **115**, 6854–6965.
39 K. J. Gagnon, H. P. Perry and A. Clearfield, Conventional and unconventional metal-organic frameworks based on phosphonate ligands: MOFs and UMOFs, *Chem. Rev.*, 2012, **112**, 1034–1054.
40 U. Schubert, Titanium-Oxo Clusters with Bi-and Tridentate Organic Ligands: Gradual Evolution of the Structures from Small to Big, *Chem.–Eur. J.*, 2021, **27**, 11239–11256.
41 U. Schubert and B. Stöger, Structural Chemistry of Titanium (IV) Oxo Clusters, Part 2: Clusters Without Carboxylate or Phosphonate Ligands, *Chem.–Eur. J.*, 2024, **30**, e202400744.
42 L. Rozes, N. Steunou, G. Fornasieri and C. Sanchez, Titanium-oxo clusters, versatile nanobuilding blocks for the design of advanced hybrid materials, *Monatsh. Chem.*, 2006, **137**, 501–528.
43 O. Auciello, W. Fan, B. Kabius, S. Saha, J. Carlisle, R. Chang, C. Lopez, E. Irene and R. Baragiola, Hybrid titanium–aluminum oxide layer as alternative high-k gate dielectric for the next generation of complementary metal–oxide–semiconductor devices, *Appl. Phys. Lett.*, 2005, **86**, 042904.
44 S. Takagi, M. Eguchi, D. A. Tryk and H. Inoue, Porphyrin photochemistry in inorganic/organic hybrid materials: Clays, layered semiconductors, nanotubes, and mesoporous materials, *J. Photochem. Photobiol., C*, 2006, **7**, 104–126.
45 L. Li, X. S. Wang, T. F. Liu and J. Ye, Titanium-based MOF materials: from crystal engineering to photocatalysis, *Small Methods*, 2020, **4**, 2000486.
46 Y.-P. Zhu, T.-Y. Ma, Y.-L. Liu, T.-Z. Ren and Z.-Y. Yuan, Metal phosphonate hybrid materials: from densely layered to hierarchically nanoporous structures, *Inorg. Chem. Front.*, 2014, **1**, 360–383.
47 S. Subudhi, S. P. Tripathy and K. Parida, Highlights of the characterization techniques on inorganic, organic (COF) and hybrid (MOF) photocatalytic semiconductors, *Catal. Sci. Technol.*, 2021, **11**, 392–415.
48 J. Panda, J. Sahu and K. Parida, Zn 0.5 Cd 0.5 Se quantum dot-integrated MOF-derived C/N–CeO 2 photocatalyst for enhanced H 2 O 2 production and O 2 evolution reactions, *Nanoscale*, 2025, **17**, 6580–6592.
49 D. Behera, P. Priyadarshini and K. Parida, ZIF-8 metal–organic frameworks and their hybrid materials: emerging photocatalysts for energy and environmental applications, *Dalton Trans.*, 2025, **54**, 2681–2708.
50 N. Priyadarshini, K. K. Das, S. Mansingh and K. Parida, Facile fabrication of functionalised Zr co-ordinated MOF: Antibiotic adsorption and insightful physiochemical characterization, *Results Chem.*, 2022, **4**, 100450.
51 R. Hayami, T. Sagawa, S. Tsukada, K. Yamamoto and T. Gunji, Synthesis, characterization and properties of titanium phosphonate clusters, *Polyhedron*, 2018, **147**, 1–8.
52 F. G. Svensson, G. Daniel, C.-W. Tai, G. A. Seisenbaeva and V. G. Kessler, Titanium phosphonate oxo-alkoxide "clusters": solution stability and facile hydrolytic transformation into nano titania, *RSC Adv.*, 2020, **10**, 6873–6883.
53 H. Li, Y. Sun, Z. Y. Yuan, Y. P. Zhu and T. Y. Ma, Titanium phosphonate based metal–organic frameworks with hierarchical porosity for enhanced photocatalytic hydrogen evolution, *Angew. Chem., Int. Ed.*, 2018, **57**, 3222–3227.
54 M. Besançon, Y. Wang, H. Mutin, J. G. Alauzun, J.-J. Robin, E. Espuche and V. Bounor-Legaré, In situ synthesis of titanium phosphonate by a non-hydrolytic sol-gel route within a viscous polymer medium, *J. Sol-Gel Sci. Technol.*, 2023, **107**, 227–243.
55 M. Pramanik, A. K. Patra and A. Bhaumik, Self-assembled titanium phosphonate nanomaterial having a mesoscopic void space and its optoelectronic application, *Dalton Trans.*, 2013, **42**, 5140–5149.
56 T.-Y. Ma, X.-J. Zhang, G.-S. Shao, J.-L. Cao and Z.-Y. Yuan, Ordered macroporous titanium phosphonate materials: synthesis, photocatalytic activity, and heavy metal ion adsorption, *J. Phys. Chem. C*, 2008, **112**, 3090–3096.

57 M. V. Vasylyev, E. J. Wachtel, R. Popovitz-Biro and R. Neumann, Titanium phosphonate porous materials constructed from dendritic tetraphosphonates, *Chem. - Eur. J.*, 2006, **12**, 3507–3514.
58 T.-Y. Ma and Z.-Y. Yuan, Functionalized periodic mesoporous titanium phosphonate monoliths with large ion exchange capacity, *Chem. Commun.*, 2010, **46**, 2325–2327.
59 T.-Y. Ma, X.-Z. Lin and Z.-Y. Yuan, Periodic mesoporous titanium phosphonate hybrid materials, *J. Mater. Chem.*, 2010, **20**, 7406–7415.
60 G. Shao, L. Lu, X. Qian and Y. Zhang, Preparation and ammonia adsorption performance of titanium phosphonate adsorbent materials with hierarchically porous structure, *J. Wuhan Univ. Technol., Mater. Sci. Ed.*, 2017, **32**, 823–829.
61 T.-Y. Ma, X.-Z. Lin, X.-J. Zhang and Z.-Y. Yuan, High surface area titanium phosphonate materials with hierarchical porosity for multi-phase adsorption, *New J. Chem.*, 2010, **34**, 1209–1216.
62 T.-Y. Ma and Z.-Y. Yuan, Periodic mesoporous titanium phosphonate spheres for high dispersion of CuO nanoparticles, *Dalton Trans.*, 2010, **39**, 9570–9578.
63 Y. P. Zhu, J. Yin, E. Abou-Hamad, X. Liu, W. Chen, T. Yao, O. F. Mohammed and H. N. Alshareef, Highly stable phosphonate-based MOFs with engineered bandgaps for efficient photocatalytic hydrogen production, *Adv. Mater.*, 2020, **32**, 1906368.
64 T. Y. Ma and S. Z. Qiao, Acid–base bifunctional periodic mesoporous metal phosphonates for synergistically and heterogeneously catalyzing CO2 conversion, *ACS Catal.*, 2014, **4**, 3847–3855.
65 B. Pawlak, W. Marchal, B. M. Ramesha, B. Joos, L. Calvi, J. D'Haen, B. Ruttens, A. Hardy, V. Meynen and P. Adriaensens, Hybrid porous titania phosphonate networks with different bridging functionalities: Synthesis, characterization, and evaluation as efficient solvent separation materials, *Microporous Mesoporous Mater.*, 2022, **341**, 112080.
66 R. Rabinowitz, The Reactions of Phosphonic Acid Esters with Acid Chlorides. A Very Mild Hydrolytic Route, *J. Org. Chem.*, 1963, **28**, 2975–2978.
67 S. N. Tverdomed, J. Kolanowski, E. Lork and G.-V. Röschenthaler, An effective synthetic route to ortho-difluoromethyl arylphosphosphonates: studies on the reactivity of phosphorus- and fluorine-containing functions, *Tetrahedron*, 2011, **67**, 3887–3903.
68 D. Wang, J. Yang, F. Xue, J. Wang and W. Hu, Experimental and computational study of zinc coordinated 1-hydroxyethylidene-1,1-diphosphonic acid self-assembled film on steel surface, *Colloids Surf., A*, 2021, **612**, 126009.
69 J. Pan, Y.-J. Ma, S.-D. Han, J.-X. Hu, Y. Mu and G.-M. Wang, Construction of the Lanthanide Diphosphonates via a Template-Synthesis Strategy: Structures, Proton Conduction, and Magnetic Behavior, *Cryst. Growth Des.*, 2019, **19**, 3045–3051.
70 J. Rocha, F. A. Almeida Paz, F.-N. Shi, R. A. S. Ferreira, T. Trindade and L. D. Carlos, Photoluminescent Porous Modular Lanthanide–Vanadium–Organic Frameworks, *Eur. J. Inorg. Chem.*, 2009, **2009**, 4931–4945.
71 F. Ishiwari, Y. Shoji and T. Fukushima, Supramolecular scaffolds enabling the controlled assembly of functional molecular units, *Chem. Sci.*, 2018, **9**, 2028–2041.
72 S. Dash, S. P. Tripathy, S. Subudhi, P. Behera, B. P. Mishra, J. Panda and K. Parida, A Visible Light-Driven α-MnO2/UiO-66-NH2 S-Scheme Photocatalyst toward Ameliorated Oxy-TCH Degradation and H2 Evolution, *Langmuir*, 2024, **40**, 4514–4530.
73 S. Dash, S. P. Tripathy, S. Subudhi, L. Acharya, A. Ray, P. Behera and K. Parida, Ag/Pd bimetallic nanoparticle-loaded Zr-MOF: an efficacious visible-light-responsive photocatalyst for H 2 O 2 and H 2 production, *Energy Adv.*, 2024, **3**, 1073–1086.
74 L. Biswal, S. P. Tripathy, S. Dash, S. Das, S. Subudhi and K. Parida, Aggrandized photocatalytic H 2 O 2 and H 2 production by a TiO 2/Ti 3 C 2–TiC/mixed metal Ce–Zr MOF composite: an interfacial engineered solid-state-mediator-based Z-scheme heterostructure, *Mater. Adv.*, 2024, **5**, 4452–4466.
75 L. Li, J. Yan, T. Wang, Z.-J. Zhao, J. Zhang, J. Gong and N. Guan, Sub-10 nm rutile titanium dioxide nanoparticles for efficient visible-light-driven photocatalytic hydrogen production, *Nat. Commun.*, 2015, **6**, 1–10.
76 J.-D. Xiao, Q. Shang, Y. Xiong, Q. Zhang, Y. Luo, S.-H. Yu and H.-L. Jiang, Boosting Photocatalytic Hydrogen Production of a Metal–Organic Framework Decorated with Platinum Nanoparticles: The Platinum Location Matters, *Angew. Chem., Int. Ed.*, 2016, **55**, 9389–9393.
77 Y. Liu, B. Zhang, L. Luo, X. Chen, Z. Wang, E. Wu, D. Su and W. Huang, TiO2/Cu2O core/ultrathin shell nanorods as efficient and stable photocatalysts for water reduction, *Angew. Chem.*, 2015, **127**, 15475–15480.
78 F. Hoffmann, M. Cornelius, J. Morell and M. Fröba, Silica-based mesoporous organic–inorganic hybrid materials, *Angew. Chem., Int. Ed.*, 2006, **45**, 3216–3251.
79 Y. Maegawa, N. Mizoshita, T. Tani and S. Inagaki, Transparent and visible-light harvesting acridone-bridged mesostructured organosilica film, *J. Mater. Chem.*, 2010, **20**, 4399–4403.
80 M. Jamshaid, A. A. Khan, K. Ahmed and M. Saleem, Heavy metal in drinking water its effect on human health and its treatment techniques-a review, *Int. J. Biosci.*, 2018, **12**, 223–240.
81 L. A. Malik, A. Bashir, A. Qureashi and A. H. Pandith, Detection and removal of heavy metal ions: a review, *Environ. Chem. Lett.*, 2019, **17**, 1495–1521.
82 A. Dutta, A. K. Patra and A. Bhaumik, Porous organic–inorganic hybrid nickel phosphonate: Adsorption and catalytic applications, *Microporous Mesoporous Mater.*, 2012, **155**, 208–214.
83 B. Maranescu, L. Lupa and A. Visa, Synthesis, characterization and rare earth elements adsorption

properties of phosphonate metal organic frameworks, *Appl. Surf. Sci.*, 2019, **481**, 83–91.
84 S. Mishra, Adsorption–desorption of heavy metal ions, *Curr. Sci.*, 2014, 601–612.
85 S. S. Gupta and K. G. Bhattacharyya, Kinetics of adsorption of metal ions on inorganic materials: a review, *Adv. Colloid Interface Sci.*, 2011, **162**, 39–58.
86 S. Dai, M. C. Burleigh, Y. Shin, C. C. Morrow, C. E. Barnes and Z. Xue, Imprint coating: a novel synthesis of selective functionalized ordered mesoporous sorbents, *Angew. Chem., Int. Ed.*, 1999, **38**, 1235–1239.
87 K. Z. Hossain and L. Mercier, Intraframework Metal Ion Adsorption in Ligand-Functionalized Mesoporous Silica, *Adv. Mater.*, 2002, **14**, 1053–1056.
88 H. Furukawa, N. Ko, Y. B. Go, N. Aratani, S. B. Choi, E. Choi, A. Ö. Yazaydin, R. Q. Snurr, M. O'Keeffe and J. Kim, Ultrahigh porosity in metal-organic frameworks, *Science*, 2010, **329**, 424–428.
89 H. Li, M. Eddaoudi, M. O'Keeffe and O. M. Yaghi, *Nature*, 1999, **402**, 276.
90 K. M. Choi, H. J. Jeon, J. K. Kang and O. M. Yaghi, Heterogeneity within order in crystals of a porous metal–organic framework, *J. Am. Chem. Soc.*, 2011, **133**, 11920–11923.
91 A. M. Furtado, J. Liu, Y. Wang and M. D. LeVan, Mesoporous silica–metal organic composite: synthesis, characterization, and ammonia adsorption, *J. Mater. Chem.*, 2011, **21**, 6698–6706.
92 S. B. Adeloju, Progress and recent advances in phosphate sensors: A review, *Talanta*, 2013, **114**, 191–203.
93 Y. Tachibana, S. A. Haque, I. P. Mercer, J. R. Durrant and D. R. Klug, Electron injection and recombination in dye sensitized nanocrystalline titanium dioxide films: a comparison of ruthenium bipyridyl and porphyrin sensitizer dyes, *J. Phys. Chem. B*, 2000, **104**, 1198–1205.
94 P. Kumar, A. Pournara, K.-H. Kim, V. Bansal, S. Rapti and M. J. Manos, Metal-organic frameworks: Challenges and opportunities for ion-exchange/sorption applications, *Prog. Mater. Sci.*, 2017, **86**, 25–74.
95 S. Sharma, A. V. Desai, B. Joarder and S. K. Ghosh, A Water-Stable Ionic MOF for the Selective Capture of Toxic Oxoanions of SeVI and AsV and Crystallographic Insight into the Ion-Exchange Mechanism, *Angew. Chem., Int. Ed.*, 2020, **59**, 7788–7792.
96 A. Bhaumik and S. Inagaki, Mesoporous titanium phosphate molecular sieves with ion-exchange capacity, *J. Am. Chem. Soc.*, 2001, **123**, 691–696.
97 X. W. Lv, C. C. Weng, Y. P. Zhu and Z. Y. Yuan, Nanoporous metal phosphonate hybrid materials as a novel platform for emerging applications: a critical review, *Small*, 2021, **17**, 2005304.
98 N. Jabeen, A. Hussain and J. Ali, in *Metal Phosphates and Phosphonates: Fundamental to Advanced Emerging Applications*, Springer, 2023, pp. 245–266.
99 P. Priyadarshini and K. Parida, Two-dimensional metal-organic frameworks and their derived materials: Properties, synthesis and application in supercapacitors field, *J. Energy Storage*, 2024, **87**, 111379.
100 D. Chakraborty, T. Dam, A. Modak, K. K. Pant, B. K. Chandra, A. Majee, A. Ghosh and A. Bhaumik, A novel crystalline nanoporous iron phosphonate based metal–organic framework as an efficient anode material for lithium ion batteries, *New J. Chem.*, 2021, **45**, 15458–15468.
101 P. Bhanja, T. Dam, S. Chatterjee, A. Bhaumik and A. Ghosh, Lithium embedded hierarchically porous aluminium phosphonate as anode material for lithium-polymer battery, *Mater. Sci. Eng., B*, 2021, **274**, 115490.
102 S. Inagaki, S. Guan, T. Ohsuna and O. Terasaki, An ordered mesoporous organosilica hybrid material with a crystal-like wall structure, *Nature*, 2002, **416**, 304–307.
103 C. Zhao, L. Ge, X. Li, M. Zuo, C. Xu, S. Chen, Q. Li, Y. Wang and C. Xu, Effects of the carbonization temperature and intermediate cooling mode on the properties of coal-based activated carbon, *Energy*, 2023, **273**, 127177.
104 A. Galarneau, M. Nader, F. Guenneau, F. Di Renzo and A. Gedeon, Understanding the Stability in Water of Mesoporous SBA-15 and MCM-41, *J. Phys. Chem. C*, 2007, **111**, 8268–8277.
105 R. Simancas, A. Chokkalingam, S. P. Elangovan, Z. Liu, T. Sano, K. Iyoki, T. Wakihara and T. Okubo, Recent progress in the improvement of hydrothermal stability of zeolites, *Chem. Sci.*, 2021, **12**, 7677–7695.
106 G. Niu, Y. Huang, X. Chen, J. He, Y. Liu and A. He, Thermal and hydrothermal stability of siliceous Y zeolite and its application to high-temperature catalytic combustion, *Appl. Catal., B*, 1999, **21**, 63–70.
107 L. P. L. Mosca, A. B. Gapan, R. A. Angeles and E. C. R. Lopez, Stability of metal–organic frameworks: recent advances and future trends, *Eng. Proc.*, 2023, **56**, 146.
108 A. J. Howarth, Y. Liu, P. Li, Z. Li, T. C. Wang, J. T. Hupp and O. K. Farha, Chemical, thermal and mechanical stabilities of metal–organic frameworks, *Nat. Rev. Mater.*, 2016, **1**, 1–15.
109 J. L. Blin, P. Riachy, C. Carteret and B. Lebeau, Thermal and hydrothermal stability of hierarchical porous silica materials, *Eur. J. Inorg. Chem.*, 2019, **2019**, 3194–3202.